Am J Transl Res 2025;17(12):9494-9515
www.ajtr.org /ISSN:1943-8141/AJTR0168783

Original Article

A set of downregulated pleiotropic genes are possible multi-omics biomarkers underlying the irritable bowel syndrome-non-alcoholic fatty liver disease comorbidity

Jundong Hong[1*], Rui Ji[2*], Peicheng Wang[1], Fengming Huang[1], Fan Zhang[3], Yanlin Zhou[4], Bin Lv[4]

[1]The First School of Clinical Medicine, Zhejiang Chinese Medical University, Hangzhou, Zhejiang, China; [2]School of Medicine, Shanghai University, Shanghai, China; [3]Zhejiang Chinese Medical University, Hangzhou, Zhejiang, China; [4]Department of Gastroenterology, The First Affiliated Hospital of Zhejiang Chinese Medical University (Zhejiang Provincial Hospital of Traditional Chinese Medicine), 54 Youdian Road, Hangzhou, Zhejiang, China. [*]Equal contributors and co-first authors.

Received September 13, 2025; Accepted November 18, 2025; Epub December 15, 2025; Published December 30, 2025

Abstract: Objective: To investigate the genetic relationship between irritable bowel syndrome (IBS) and non-alcoholic fatty liver disease (NAFLD). Methods: Mendelian randomization (MR) was used to assess causality between IBS and NAFLD in a genome-wide association study (GWAS) data. Genetic correlation was evaluated by linkage disequilibrium score regression (LDSC). Shared loci were identified using PLACO, coloc, and MAGMA for pleiotropic gene mapping. Functional enrichment (Gene Ontology [GO]/Kyoto Encyclopedia of Genes and Genomes [KEGG]) was performed. Single-cell RNA-sequencing of NAFLD liver samples was used to assess gene dysregulation and calculate activation scores. Mouse models were used to validate gene expression. The identified pleiotropic gene set and their dysregulation signatures provide a foundational resource for future development of predictive multi-omics biomarkers. Results: MR revealed a significant causal effect of IBS on NAFLD risk (Inverse-variance weighted: OR = 1.118, 95% CI = 1.03-1.21, P = 0.006; Steiger P < 0.05). Significant genetic correlation was observed (LDSC P < 0.05). Analyses identified 194 pleiotropic SNPs, mapping to 12 genes (e.g., *GCKR, ARHGAP25, SNX17*). These genes were enriched in nucleotide, carbohydrate, and lipid metabolism pathways. Tissue-specific analysis indicated a decreased activation pattern of pleiotropic genes in the liver tissues. Single-cell analysis showed dysregulation in NAFLD hepatocytes/immune cells. In addition, activation scores negatively correlated with disease severity (P < 0.001). Mouse models confirmed overall downregulation of these genes, significant for *GCKR*, *GPN1*, and *SLC4A1AP* at both mRNA and protein levels. Conclusions: IBS exhibits a unidirectional causal effect on NAFLD, and there is a significant genetic association between them. The collective downregulation of shared pleiotropic genes (*ADCY2, ARHGAP25, C2orf16, CCDC121, GCKR, GPN1, LINC01460, SLC4A1AP, SNX17, ZNF512, ZNF513*, and *EIF2B4*) may mediate increased susceptibility to NAFLD in the IBS population.

Keywords: Irritable bowel syndrome, non-alcoholic fatty liver disease, genetic correlation, pleiotropy

Introduction

Irritable Bowel Syndrome (IBS) is a chronic functional disorder characterized by abdominal pain and altered bowel function, with a global prevalence of approximately 10% [1]. Patients often experience extra-intestinal manifestations, such as musculoskeletal pain, chronic fatigue, anxiety, and depression [2-4], and the condition may be related to mechanisms such as abnormal immune responses, gut microbiota imbalances, and disruptions in the brain-gut axis [5]. Non-alcoholic fatty liver disease (NAFLD), also referred to as metabolic dysfunction-associated fatty liver disease (MASLD), is defined as lipid accumulation in the liver, excluding alcohol (women < 20 g/day, men < 30 g/day) and other secondary causes [6]. NAFLD patients are at risk for various adverse clinical outcomes, with liver fibrosis being the primary one, ultimately leading to cirrhosis, liver cancer, and other complications [7-9]. Epidemiologic studies have clearly confirmed the association between IBS and NAFLD.

https://doi.org/10.62347/KPGF8790

Among IBS patients, 65.8% to 74.0% develop NAFLD, while nearly 23.2% to 29.4% of NAFLD patients display IBS-like symptoms [10]. Studies suggest a similar pathogenesis between IBS and NAFLD, such as upregulated inflammatory factors, gut microbiota dysbiosis, and intestinal barrier dysfunction [11].

Furthermore, studies have shown that patients with IBS are more likely to have metabolic syndrome, which is generally considered to be associated with the onset of NAFLD [12-14]. However, the temporal relationship remains unclear, highlighting the need for further investigation.

This study investigates whether the co-occurrence of IBS and NAFLD is a coincidental comorbidity or causal association. By employing two-sample Mendelian randomization, genetic correlation analyses, pleiotropic gene mapping, and functional enrichment, coupled with single-cell transcriptomic profiling of NAFLD livers and validation in mouse models, this study elucidated the causal relationship and underlying molecular mechanisms between IBS and NAFLD. These findings provide novel insight into disease management while establishing potential therapeutic targets for clinical intervention.

Materials and methods

Causal analysis

To assess the causal relationship between IBS and NAFLD, we first performed a two-sample Mendelian analysis using Genome-wide association study (GWAS) data for IBS and NAFLD. Mendelian analysis is a genetic variant-based causal inference method widely used to investigate exposure-outcome relationships [15]. The GWAS datasets for IBS and NAFLD (Single Nucleotide Polymorphism (SNP) datasets) were obtained from the GWAS Catalog, an authoritative repository that systematically collects, standardizes and disseminates published genome-wide association study findings globally. The IBS dataset comprised 24,735 patients meeting ROME III criteria from two independent European cohorts (UK Biobank and Lifelines), along with 77,149 healthy controls [16]. The NAFLD dataset included 8,438 European NAFLD patients and 770,180 healthy controls [17]. As the data were derived from publicly available databases, no additional ethical approval was required.

Analyses were conducted using the two-sample Mendelian Randomization (MR) package, with instrument selection at $P < 1.0 \times 10^{-5}$. Independent SNPs were clumped using genomic data from European population as a reference (linkage disequilibrium threshold: $R^2 < 0.001$; window size: 10,000 kb). Causal estimates were derived through three complementary methods: inverse-variance weighted (IVW) as the primary analysis, supplemented by MR-Egger regression and weighted median approaches. The IVW method provided the most precise estimates under valid instrument assumptions. The Steiger test was applied to validate causal directionality.

Genomic genetic association analysis

LD score regression (LDSC), a method based on GWAS data, calculates the genetic correlation coefficient (rg) between traits, quantifying shared genetic risk factors to delineate the genetic architecture of complex traits [18]. In this study, LDSC was performed using the GenomicSEM package in R to evaluate the genetic association between IBS and NAFLD.

Detection of pleiotropy SNPs

Pleiotropy Analysis with Collapsing (PLACO) was used to identify pleiotropy SNPs between IBS and NAFLD [19]. Additionally, colocalization analysis by the R coloc package was applied to detect shared pleiotropic genes between IBS and NAFLD. Furthermore, multi-marker analysis of GenoMic annotation (MAGMA) based on GWAS data was employed for functional annotation of pleiotropic SNPs to match corresponding genes [20]. All identified SNPs underwent false discovery rate (FDR) correction, with FDR-adjusted $P < 0.05$ considered significant for pleiotropy.

Annotation of biological gene functions

We conducted Gene Ontology (GO) and Kyoto Encyclopedia of Genes and Genomes (KEGG) enrichment analyses of related pleiotropic genes. The GO analysis leverages standardized ontological vocabulary to annotate target genes across three domains: Molecular Function (MF), Biological Process (BP), and Cellular Component (CC). KEGG pathway analysis focuses on deciphering coordinated gene actions within metabolic pathways and signal transduc-

tion networks, identifying significantly enriched pathways to elucidate possible mechanisms underlying specific phenotypes or diseases. Functional Mapping and Annotation (FUMA) platform was employed for tissue-specific expression profiling of pleiotropic genes.

Gene expression analysis

To further investigate the role of pleiotropic genes in hepatic steatosis, their expression patterns were validated using The *NAFLD Single-cell RNA Sequencing (scRNA-seq) Database (https://dreamapp.biomed.au.dk/NAFLD-scRNA-seq/)* provided by Wenfeng Ma et al., which incorporates transcriptional profiles from 82 liver and peripheral blood mononuclear cell (PBMC) specimens [21]. The specific expression patterns were also verified across cell types, tissues, and disease states. Additionally, the GSE202379 dataset, which contains 47 samples yet to be included in *NAFLD scRNA seq Database*, was analyzed to assess clinical relevance [22]. The analysis was conducted using the Seurat R package [23]. Nuclei fewer than 200 or more than 50,000 counts, over 25% mitochondrial gene content, or containing erythrocyte genes were excluded. Subsequently, sample integration was performed using the Harmony R package [24]. The raw data were first normalized using *NormalizeData*, and highly variable genes were identified with *FindVariableFeatures*. Based on these genes, dimensionality reduction was conducted using Principal Component Analysis (PCA), followed by batch effect correction with *RunHarmony*. Neighbor detection was performed using *FindNeighbors* with dims = 1:15, and clustering was done using *FindClusters* with resolution = 0.5. Cell markers from the original publication guided subcluster annotation, and Uniform Manifold Approximation and Projection (UMAP) visualization was generated using the *scRNAtoolVis* package.

AUCell R package [25] was employed to quantify genome-wide activation levels of key genes. Cells were stratified into high- and low-activity groups using empirically determined activation thresholds, followed by differential analysis by the *FindMarkers()* function. Pathway activity states in lipogenic pathways were compared between groups using Gene Set Enrichment Analysis (GSEA) base [26]. Finally, Pearson correlation analysis ($\alpha = 0.05$, two-sided) was used to evaluate clinical correlations between Area Under Curve (AUC) scores and NAFLD progression metrics, including disease stage, fibrosis severity, inflammatory activity, and Steatosis-Activity-Fibrosis (SAF) scores.

Animals and experimental design

Female C57BL/6 mice (6-8 weeks old) were purchased from Shanghai Sippr-BK Laboratory Animal Co., Ltd. Mice were randomly allocated into a control group (n = 15) and an experimental group (n = 30), housed in polycarbonate cages (5 per cage) under standard conditions (temperature: 20°C-23°C; humidity: 22.7%-66.8%). All mice had *ad libitum* access to food and water. After a one-week acclimatization period, the experimental group was subjected to daily restraint stress to establish the diarrhea-predominant IBS (IBS-D) mice model. Specifically, mice were restrained in 50 mL conical centrifuge tubes for 2 hours starting at 11:30 AM, while the control group received no intervention. Body weight and stool consistency were recorded daily prior to restraint initiation. The restraint intervention lasted 14 consecutive days. Behavioral changes were assessed using the Open Field Test (OFT) on day 15. Subsequently, liver samples were collected for Oil Red O staining to evaluate hepatic steatosis and quantitative reverse transcription polymerase chain reaction (RT-qPCR) to analyze the expression of pleiotropic genes. All animal experiments were approved by the Animal Ethics Committee of Zhejiang Chinese Medical University and were conducted with efforts to minimize animal suffering.

Open field test: Mice behavior was recorded and analyzed using Panlab Smart v3.0.06. Mice were acclimated to a dark, open-field arena (1 m × 1 m, divided into 16 zones) for 20 seconds, followed by 5-minute movement recording. Zones 6, 7, 10, and 11 were defined as the central area, while the remaining zones were designated as peripheral regions.

Oil red O staining: After cervical dislocation, liver tissues were immediately excised, rinsed with ice-cold PBS, blotted dry, and flash-frozen on dry ice. Cryostat sections (-20°C) were prepared, fixed on pre-treated slides, and stained with Oil Red O (5-minute 70% ethanol pre-treatment, 15-minute staining). Sections were counterstained with hematoxylin (1 minute), rinsed,

Table 1. RT-qPCR gene primers

Human Gene	Mouse Gene	Direction	Sequence (5' to 3')
GCKR	GCKR	Front	AGGCATTTCCGTGGGACTCTC
		Reverse	ACCGGATTGAAGCCAACCAG
SNX17	SNX17	Front	CGAACCTGGTAGTACGGAGC
		Reverse	CTCCTTCCGAAGCACGTAGG
ARHGAP25	ARHGAP25	Front	AGGCTTCAAAAATAGGGCTGC
		Reverse	ATTTCCCAGCTTCTTCGGGG
ADCY2	ADCY2	Front	GGAGCCTGAAAAACGAGGAGT
		Reverse	GAGGCATTCCAAGCCTTCCT
C2orf16/SPATA31H1	C2orf16/SPATA31H1	Front	GTTATCGCAGCCGAACACAG
		Reverse	TCCATAAGTGCTGAGCTTGC
CCDC121	CCDC121	Front	AGTTCTGGAACCAGGTTTGCC
		Reverse	ACGTTGATGGCTGAGGAGAAC
EIF2B4	EIF2B4	Front	GCTGTTCGCGAAGTGCGTC
		Reverse	GAGGACTTGGGGAGACTCGT
GPN1	GPN1	Front	GAGCTAGGATTTGCCCTGGT
		Reverse	TAAGAACTGCCTGGCTCGTG
SLC4A1AP	SLC4A1AP	Front	GGCAAAATAGTGTCGTCATGTG
		Reverse	TATTCATTCGCTGGTGCTGCT
ZNF512	zfp512	Front	TGCATGCGTGAGGTCTTCTT
		Reverse	AGGTAACCCAGGGCGAGTAT
ZNF513	zfp513	Front	GGGAGGGAGATTCCACAAGC
		Reverse	CCCCTGAGAGTCTCCTTCAGA
Actb	Actb	Front	TCCGGCACTACCGAGTTATC
		Reverse	GATCCGGTGTAGCAGATCGC

RT-qPCR: Reverse transcription quantitative polymerase chain reaction, ADCY2: Adenylate Cyclase 2, Actb: Beta-Actin, C2orf16/SPATA31H1: Chromosome 2 Open Reading Frame 16/Spermatogenesis Associated 31 Member H1, CCDC121: Coiled-Coil Domain Containing 121, EIF2B4: Eukaryotic Translation Initiation Factor 2B Subunit Beta, GCKR: Glucokinase Regulator, GPN1: GPN-Loop GTPase 1, LINC01460: Long Intergenic Non-Protein Coding RNA 1460, ARHGAP25: Rho GTPase Activating Protein 25, SLC4A1AP: SLC4A1 Associated Pseudogene, SNX17: Sorting Nexin 17, ZNF512: Zinc Finger Protein 512, ZNF513: Zinc Finger Protein 513, zfp512: zinc finger protein 512, zfp513: zinc finger protein 513.

mounted with glycerin gelatin, and imaged under an optical microscope.

RT-qPCR: Total RNA was extracted from liver tissues using the AccurateBio SteadyPure RNA Extraction Kit (AG21024) and reverse-transcribed into cDNA with the YEASEN Hifair® II 1st Strand cDNA Synthesis Kit (11141ES60). RT-qPCR was performed using YEASEN Hieff® qPCR SYBR Green Master Mix (1120ES08) on a Thermo Fisher ABI 7900 system (10 μL reaction volume, three technical replicates). Primer sequences (**Table 1**) were validated by Primer-BLAST, with *Actb* as the reference gene. Data were analyzed using the 2-ΔΔCt method in R, with visualizations generated by *ggplot2*. Normality was assessed using Shapiro-Wilk tests, and group differences were evaluated using a two-tailed Student's t-test ($P < 0.05$ deemed significant).

Western blot: Liver tissues were homogenized using a tissue grinder at 4°C, followed by protein extraction with RIPA buffer containing PMSF protease inhibitor. The protein homogenate was centrifuged at 12,000 rpm under low temperatures, and the supernatant was carefully collected. Target proteins were separated by sodium dodecyl sulfate-polyacrylamide gel electrophoresis (SDS-PAGE) and transferred onto polyvinylidene fluoride (PVDF) membranes. The membranes were then incubated with a blocking solution at 37°C for 2 hours. Subsequently, the membranes were incubated overnight at 4°C with corresponding specific primary antibodies, followed by incubation with

appropriate secondary antibodies for 2 hours. Target proteins were detected using an enhanced diaminobenzidine (DAB) solution, and grayscale values were analyzed using ImageJ. The experiment was conducted in triplicates.

Antibodies used included GCKR (Zenbio, 822411, 1:1000), ADCY2 (Affinity Biosciences, DF2270, 1:300), SLC4A1AP (Immunoway, YT2499, 1:1000), ARHGAP25 (Proteintech, 14349-1-AP, 1:1000), ZNF512 (Proteintech, 24508-1-AP, 1:500), GPN1 (Proteintech, 15-752-1-AP, 1:1000), α-Tubulin (Proteintech, 11224-1-AP, 1:20000), Goat Anti-Rabbit IgG H&L (HRP) (Zenbio, 511203, 1:10000).

Statistical analysis

All statistical analyses were conducted using R software (v4.4.2). The specific statistical methods applied in each analytical step of this study are detailed in their respective sections. In brief, causal inference in Mendelian randomization (MR) relied primarily on the inverse-variance weighted (IVW) method, with sensitivity analyses performed using MR-Egger and weighted median approaches, with a *P*-value < 0.05 considered significant. Genetic correlation was assessed using LD Score regression (LDSC). For pleiotropy analysis, a false discovery rate (FDR) correction was applied (FDR < 0.05 deemed significant). Functional enrichment analysis of genes also utilized FDR correction. In scRNA-seq data analysis, differential expression was evaluated using the Wilcoxon rank-sum test, and correlations were assessed by Pearson's method. For validation experiments in mouse models, group differences were analyzed using a two-tailed Student's t-test, with a *P*-value < 0.05 considered significant.

Package version

The software and corresponding versions used in our study are listed below: R (v4.4.2), TwoSampleMR package (v0.5.7), GenomicSEM R package (v0.0.5), PLACO (v0.1.1), coloc R package (v5.2.3), MAGMA (v1.1.0), Seurat R package (v5.1.0), harmony R package (version 1.2.1), scRNAtoolVis (v0.1.0), AUCell R package (v1.26.0), GSEABase (version 1.66.0), GSEABase (v1.66.0).

Results

Causality analysis

After data filtering, 90 SNPs were selected for two-sample Mendelian analysis. IVW suggested a significant causal association between IBS and NAFLD (OR = 1.12, 95% CI = 1.03-1.21, *P* = 0.006). MR-Egger (OR = 1.0353, 95% CI = 0.962-1.114) and weighted median (OR = 1.0380, 95% CI = 1.006-1.071) showed consistent directionality. MR-Steiger directionality testing suggested a unidirectional causal relationship from IBS to NAFLD. Directional pleiotropy was tested using the MR-Egger intercept test, which suggested no directional pleiotropy (P = 0.52). Heterogeneity analysis with Cochran's Q test revealed heterogeneity in the results (IVW P = 0.0403, MR-egger P = 0.0371). We then performed cyclic calculation using MR-PRESSO to remove outlier SNPs, with 5000 times for each simulation, until no further outliers were detected. The above analysis was performed after removing all outlier SNPs, and the results were robust, suggesting a unidirectional causal association of IBS with NAFLD. The overall study workflow is summarized in **Figure 1**, and **Figure 2** presents the detailed results of the Mendelian analysis.

LDSC genetic association analysis

Based on the hypothesis that IBS and NAFLD share a common genetic architecture, and after excluding SNPs with a minor allele frequency (MAF) > 5%, LDSC was performed to assess the genetic correlation between IBS and NAFLD datasets. This analysis revealed a significant genetic correlation (rg = 27.16% ± 13.57%, P = 0.0453). Notably, SNP-based heritability (h^2) estimates differed substantially between traits: 7.51% for IBS compared to 0.14% for NAFLD, suggesting that non-genetic factors (e.g., environmental influences) predominantly contribute to NAFLD pathogenesis.

Annotation of pleiotropy gene

Pleiotropy SNPs between IBS and NAFLD were identified using Pleiotropy Analysis under Composite Null (PLACO). Colocalization analysis further pinpointed shared genomic regions. SNPs surviving FDR adjustment (*P* < 0.05) were considered pleiotropic. Gene-based functional

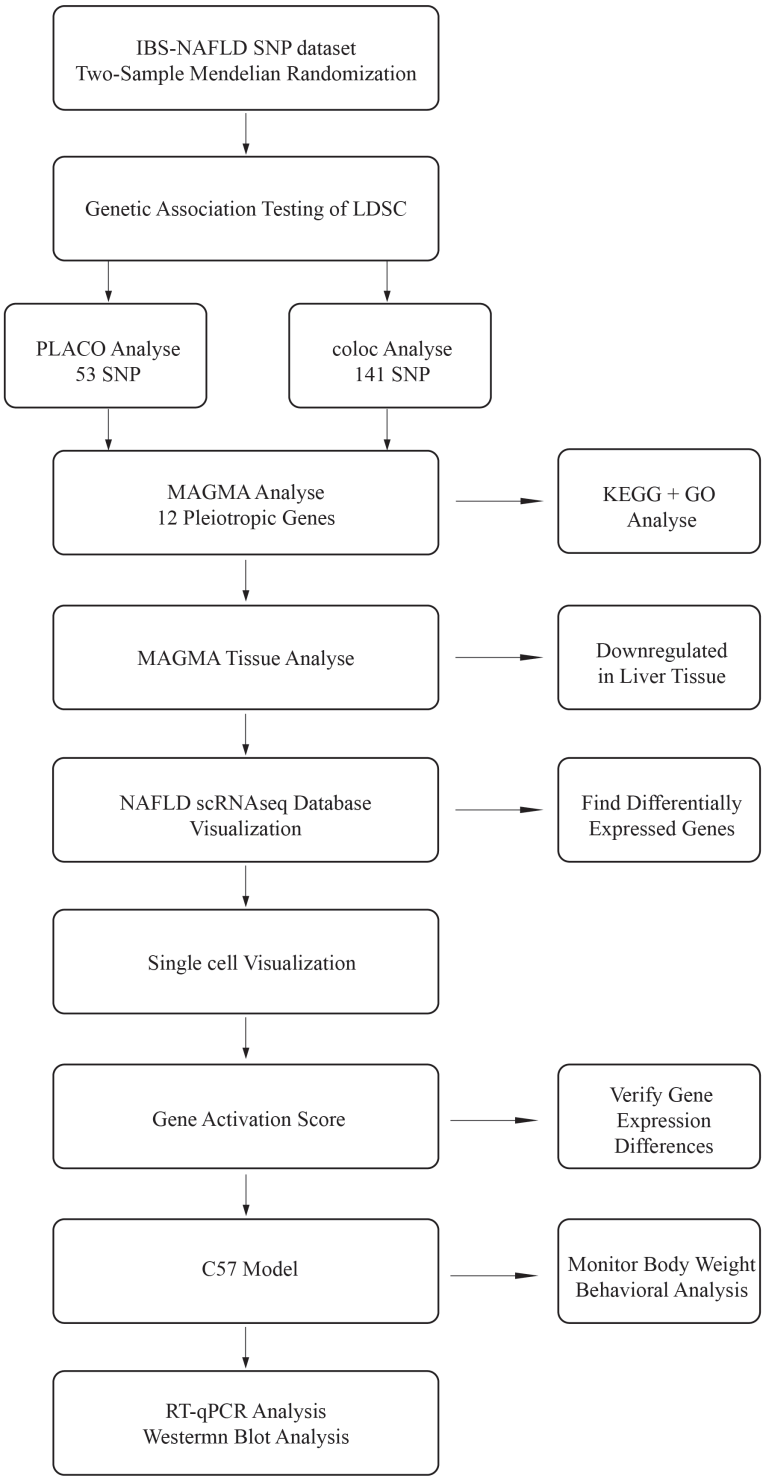

Figure 1. Study flowchart. IBS: Irritable Bowel Syndrome, NAFLD: Non-Alcoholic Fatty Liver Disease, LDSC: LD Score regression, PLACO: Pleiotropy Analysis with Collapsing, coloc: colocalization, MAGMA: Multi-marker Analysis of GenoMic Annotation, GO: Gene Ontology, KEGG: Kyoto Encyclopedia of Genes and Genomes, scRNA-seq: Single-cell RNA, RT-qPCR: reverse transcription quantitative polymerase chain reaction.

annotation was performed using Multi-marker Analysis of GenoMic Annotation (MAGMA), mapping SNPs to genes (window: ±10 kb). After FDR correction ($P < 0.05$), 13 candidate genes were identified. Following the exclusion of one pseudogene (ENSG00000233438), 12 genes (Adenylate Cyclase 2 (ADCY2), Rho GTPase Activating Protein 25 (ARHGAP25), Chromosome 2 Open Reading Frame 16/Spermatogenesis Associated 31 Member H1 (C2orf16/SPATA31H1), Coiled-Coil Domain Containing 121 (CCDC121), Glucokinase Regulator (GCKR), GPN-Loop GTPase 1 (GPN1), Long Intergenic Non-Protein Coding RNA 1460 (LINC01460), SLC4A1 Pseudogene (SLC4A1P), Sorting Nexin 17 (SNX17), Zinc Finger Protein 512 (ZNF512), Zinc Finger Protein 513 (ZNF513)) with validated biological relevance were retained. Detailed gene characteristics are summarized in **Table 2**.

Functional enrichment of pleiotropic genes

Gene functions were investigated using GO and KEGG pathway enrichment analyses. In GO analysis, we focused on BP and MF levels. At the BP level (**Figure 3**), four pleiotropic genes (*ADCY2, GCKR, SNX17* and *EIF2B4*) showed significant effects, mainly enriched in cAMP metabolome, cholesterol metabolome, and glucose metabolome, including cAMP biosynthesis, cholesterol catabolism, glucokinase activity regulation, carbohydrate response, forskolin response, response to fructose, response

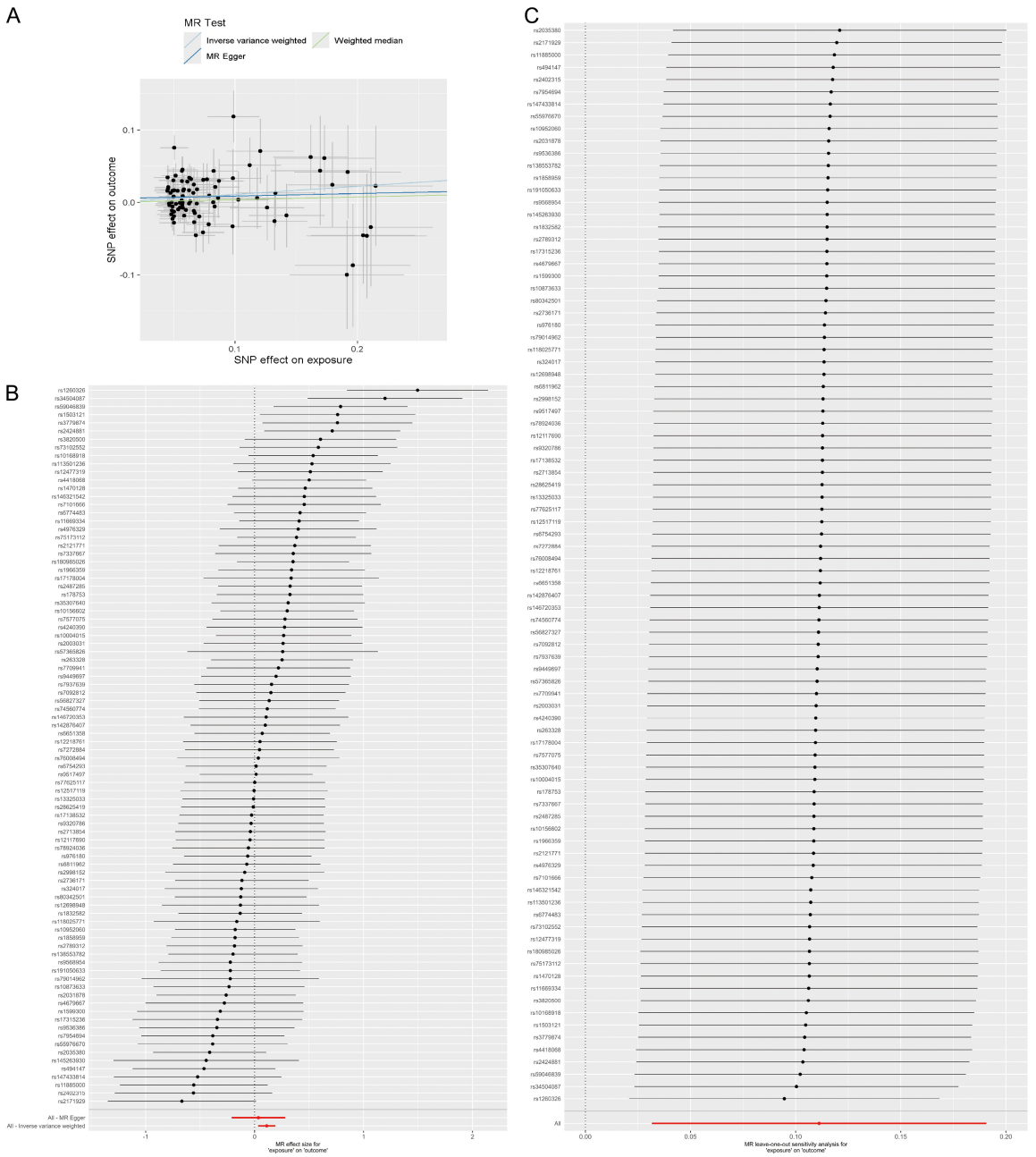

Figure 2. Two-sample Mendelian results for the IBS versus NAFLD dataset. A. Effect plots of MR Egger, IVW, and Weight Median methods, showing consistent trend; B. Forest plot of Mendelian randomization, showing the influence of each SNP and the combined effect on the results; C. Leave-one-out method plot of Mendelian randomization, showing the changes in the results after removing each SNP, none of which had a significant effect on the results after removal. IBS: Irritable Bowel Syndrome, NAFLD: Non-Alcoholic Fatty Liver Disease, IVW: inverse-variance weighted, SNP: Single Nucleotide Polymorphism.

to hexose, response to monosaccharides and sterol catabolism. At the MF level (**Figure 9C**), four pleiotropic genes were significant (*ARHGAP25, EIF2B4, ADCY2* and *SNX17*), involving adenylyl cyclase activity regulation, adenylyl cyclase binding, cyclase activity, phosphorylase activity, low-density lipoprotein particle receptor binding, lipoprotein particle receptor binding, translation initiation factor binding and activity, GTPase activator activity and regulator activity. KEGG pathway enrichment analysis (**Figure 4**) identified *ADCY2* as the key enriched gene, and the pathways involved included ovarian steroidogenesis, adipocyte lipolysis regula-

Table 2. IBS and NAFLD pleiotropic genes

ENE	CHR	START	STOP	P	SYMBOL
ENSG00000078295	5	7391321	7835194	0.040223	ADCY2
ENSG00000163219	2	68901733	69058965	0.015122	ARHGAP25
ENSG00000221843	2	27794389	27810588	0.015684	C2orf16
ENSG00000176714	2	27843506	27856879	0.018757	CCDC121
ENSG00000084734	2	27714709	27751554	0.002047	GCKR
ENSG00000198522	2	27846114	27879375	0.018757	GPN1
ENSG00000205334	2	27923653	27943599	0.015198	LINC01460
ENSG00000163798	2	27881338	27922840	0.015227	SLC4A1AP
ENSG00000115234	2	27588389	27604995	0.015227	SNX17
ENSG00000243943	2	27800897	27863041	0.014989	ZNF512
ENSG00000163795	2	27595098	27608657	0.015227	ZNF513
ENSG00000115211	2	27582219	27598353	0.015227	EIF2B4

We matched the pleiotropy genes through MAGMA and identified 12 pleiotropy genes (*ADCY2, ARHGAP25, C2orf16, CCDC121, GCKR, GPN1, LINC01460, SLC4A1AP, SNX17, ZNF512, ZNF513* and *EIF2B4).* IBS: Irritable Bowel Syndrome, NAFLD: Non-Alcoholic Fatty Liver Disease, RT-qPCR: Reverse transcription quantitative polymerase chain reaction, MAGMA: Multi-marker Analysis of GenoMic Annotation, ADCY2: Adenylate Cyclase 2, Actb: Beta-Actin, C2orf16/SPATA31H1: Chromosome 2 Open Reading Frame 16/Spermatogenesis Associated 31 Member H1, CCDC121: Coiled-Coil Domain Containing 121, EIF2B4: Eukaryotic Translation Initiation Factor 2B Subunit Beta, GCKR: Glucokinase Regulator, GPN1: GPN-Loop GTPase 1, LINC01460: Long Intergenic Non-Protein Coding RNA 1460, ARHGAP25: Rho GTPase Activating Protein 25, SLC4A1AP: SLC4A1 Associated Pseudogene, SNX17: Sorting Nexin 17, ZNF512: Zinc Finger Protein 512.

tion, longevity regulation, cortisol synthesis and secretion, thyroid hormone synthesis, gastric acid secretion, insulin secretion, Gamma-aminobutyric acid (GABA) aminobutyric acid synapse, bile secretion and other physiological processes. This suggests that multiple pathways mediate the biological processes in the pathogenesis of NAFLD in IBS patients.

Tissue function identification of pleiotropic genes

The co-pathogenesis of IBS and NAFLD may involve specific organs or tissues. The MAGMA tissue method was used to analyze the comprehensive expression of the obtained genes in 54 tissues. Although the significance threshold was not reached, tissue enrichment analysis showed that pleiotropic genes were highly expressed in tissues such as the liver and heart. An overall downward trend in the expression of pleiotropic genes was observed in the liver (**Figure 5**). To further analyze the role of these genes in tissues, we analyzed their expression in liver tissues using the NAFLD scRNA-seq database. **Figure 6A-D** show the visualization of the expression of some pleiotropic genes (e.g., *ARHGAP25, GCKR* and *SNX17*) in the cell population. The expression of other genes is shown in Supplementary Figure 1. Among the pleiotropic genes, *GCKR* was highly expressed in bile duct cells and hepatocytes, *ARHGAP25* was highly expressed in intrahepatic macrophages, and *SLC4A1AP* and *GPN1* were highly expressed in peripheral NK cells (**Figure 6E**). The expression patterns varied among disease states and tissues, such as the low expression of *ARHGAP25, GPN1*, and *SNX17* in NAFLD and the expression preferences in peripheral immune cell subsets. Further analysis quantified these observations, confirming that the expression of pleiotropic genes was altered not only in NAFLD compared to controls (**Figure 6F**) but also between hepatic and peripheral immune cells (**Figure 6G**).

We then visualized the cellular composition of different segments of NAFLD and obtained the corresponding marker genes in GSE202379 (**Figure 7A**, **7B**). The expression of pleiotropic genes was further validated, with *GCKR* being highly expressed in hepatocytes, and *ARHGAP25* highly expressed in macrophages, neutrophils, and lymphocytes (**Figure 7C**). Cells were categorized into high- and low-activation groups according to the AUCell threshold (**Figure 7D**, **7E**), and a difference analysis was performed. GSEA results showed that compared with the high-activation group, the low-activation group showed an up-regula-

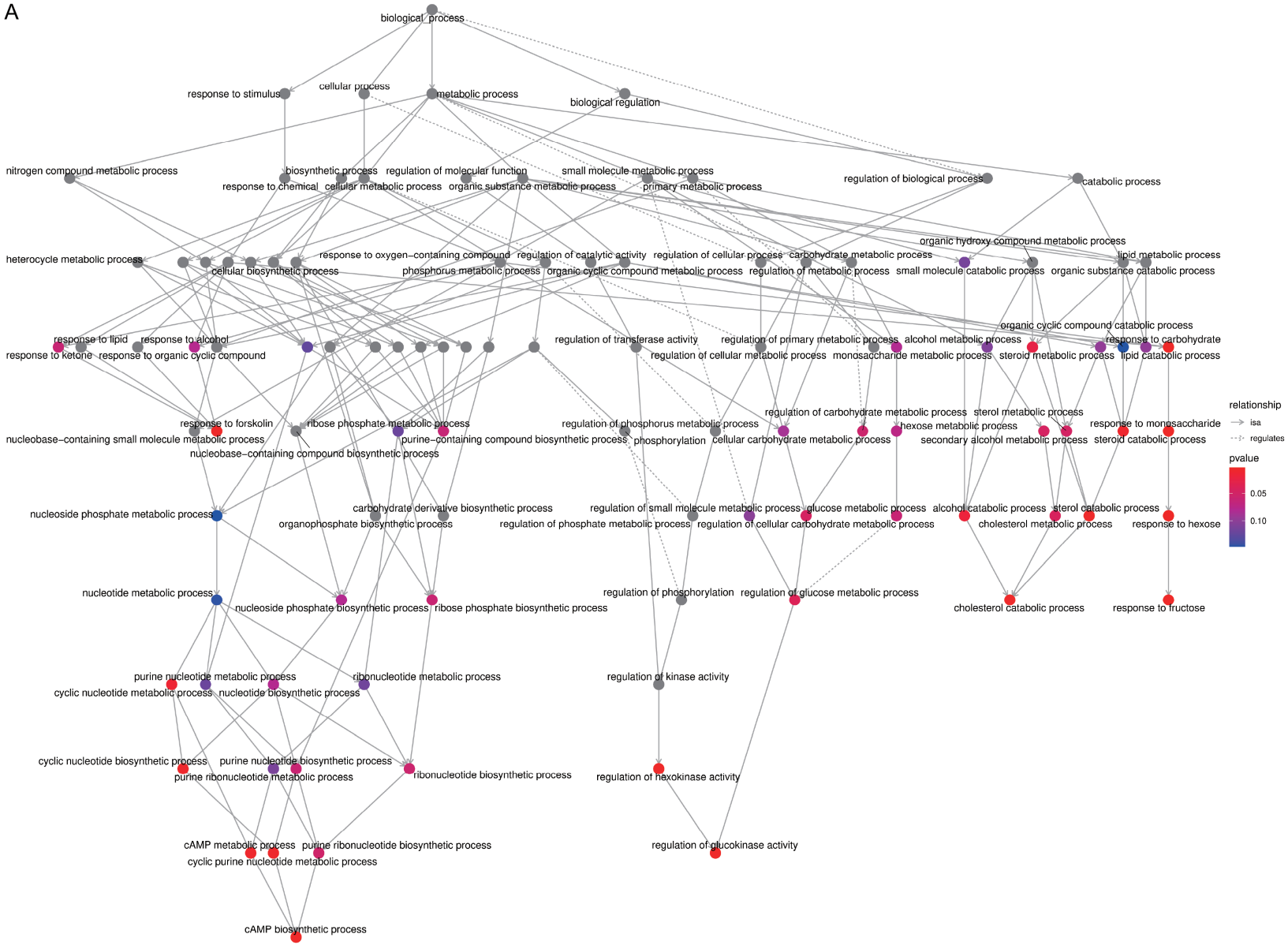
A
biological_process
response to stimulus
cellular process
metabolic process
biological regulation
nitrogen compound metabolic process
biosynthetic process
regulation of molecular function
small molecule metabolic process
regulation of biological process
catabolic process
response to chemical
cellular metabolic process
organic substance metabolic process
primary metabolic process
organic hydroxy compound metabolic process
heterocycle metabolic process
response to oxygen−containing compound
regulation of catalytic activity
regulation of cellular process
carbohydrate metabolic process
lipid metabolic process
cellular biosynthetic process
phosphorus metabolic process
organic cyclic compound metabolic process
regulation of metabolic process
small molecule catabolic process
organic substance catabolic process
organic cyclic compound catabolic process
response to lipid
response to alcohol
regulation of transferase activity
regulation of primary metabolic process
alcohol metabolic process
response to carbohydrate
response to ketone
response to organic cyclic compound
regulation of cellular metabolic process
monosaccharide metabolic process
steroid metabolic process
lipid catabolic process
regulation of carbohydrate metabolic process
sterol metabolic process
response to forskolin
ribose phosphate metabolic process
regulation of phosphorus metabolic process
hexose metabolic process
response to monosaccharide
nucleobase−containing small molecule metabolic process
purine−containing compound biosynthetic process
phosphorylation
cellular carbohydrate metabolic process
secondary alcohol metabolic process
steroid catabolic process
nucleobase−containing compound biosynthetic process
relationship
isa
regulates
pvalue
0.05
0.10
nucleoside phosphate metabolic process
carbohydrate derivative biosynthetic process
regulation of small molecule metabolic process
glucose metabolic process
alcohol catabolic process
sterol catabolic process
organophosphate biosynthetic process
regulation of phosphate metabolic process
regulation of cellular carbohydrate metabolic process
cholesterol metabolic process
response to hexose
nucleotide metabolic process
regulation of phosphorylation
regulation of glucose metabolic process
nucleoside phosphate biosynthetic process
ribose phosphate biosynthetic process
cholesterol catabolic process
response to fructose
purine nucleotide metabolic process
ribonucleotide metabolic process
regulation of kinase activity
cyclic nucleotide metabolic process
nucleotide biosynthetic process
cyclic nucleotide biosynthetic process
purine nucleotide biosynthetic process
ribonucleotide biosynthetic process
purine ribonucleotide metabolic process
regulation of hexokinase activity
cAMP metabolic process
purine ribonucleotide biosynthetic process
regulation of glucokinase activity
cyclic purine nucleotide metabolic process
cAMP biosynthetic process

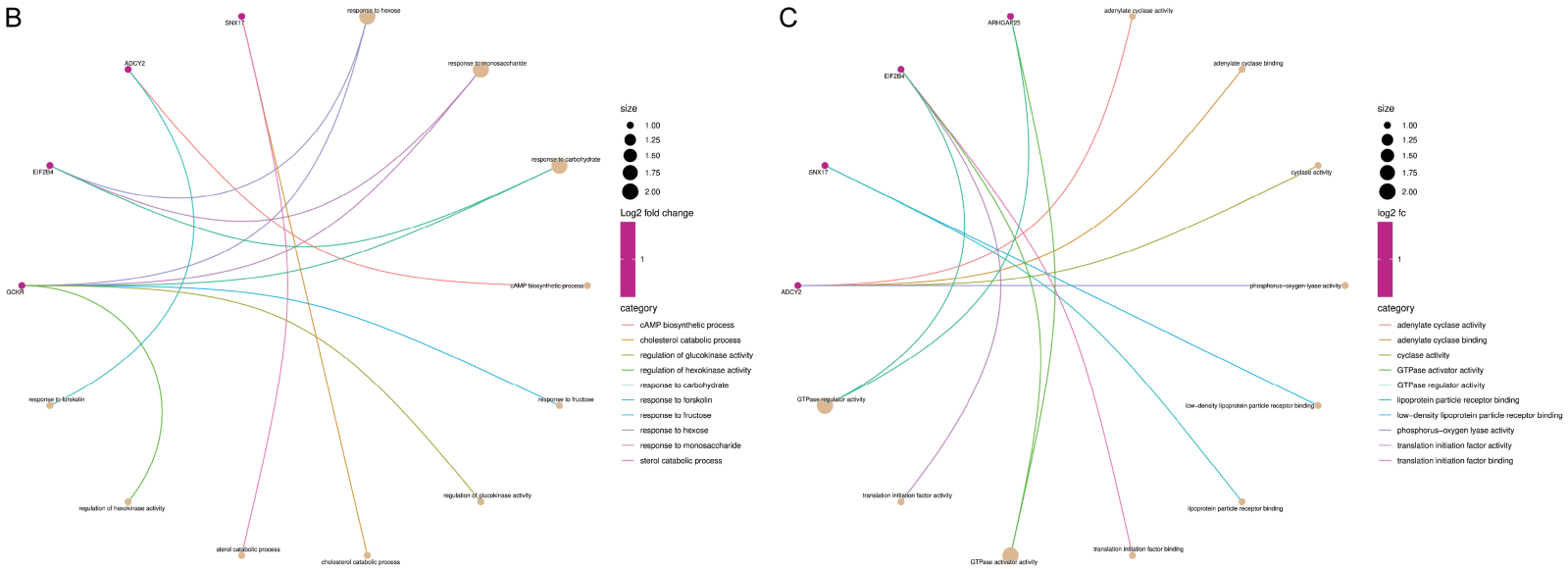

Figure 3. Biological process and molecular function of GO analysis of pleiotropic genes. A. Directed acyclic graph of biological functions of pleiotropic genes, showing the interaction of biological functions affected by pleiotropic genes; B. Association between enriched genes and functions in terms of BP; C. Links between enriched genes and functions in terms of MF. GO: Gene Ontology, MF: Molecular Function, BP: Biological Process.

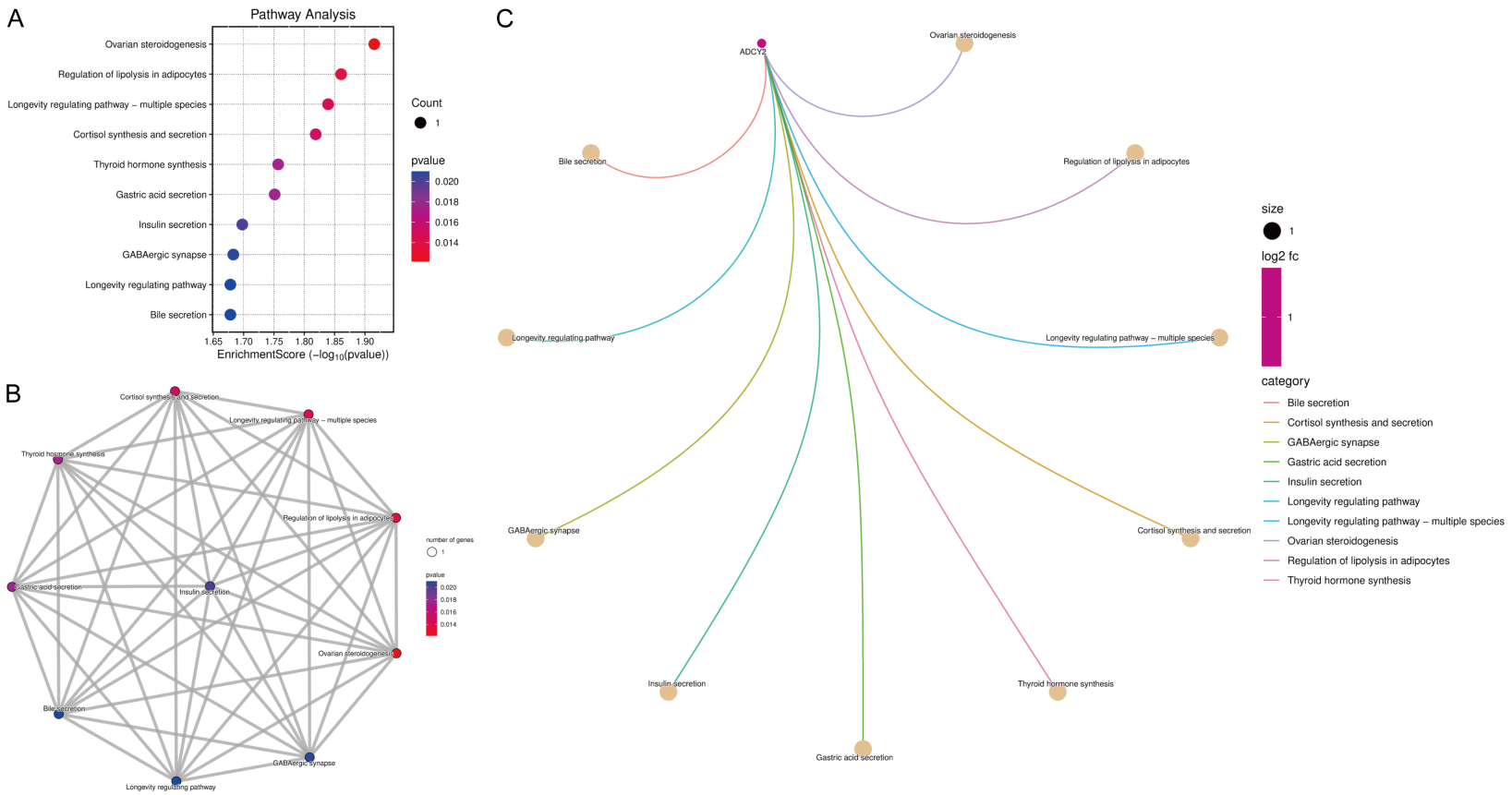

Figure 4. KEGG analysis of pleiotropic genes. A. KEGG biological function enrichment map; B. KEGG biological function association diagram; C. Enriched gene and functional association map. KEGG: Kyoto Encyclopedia of Genes and Genomes.

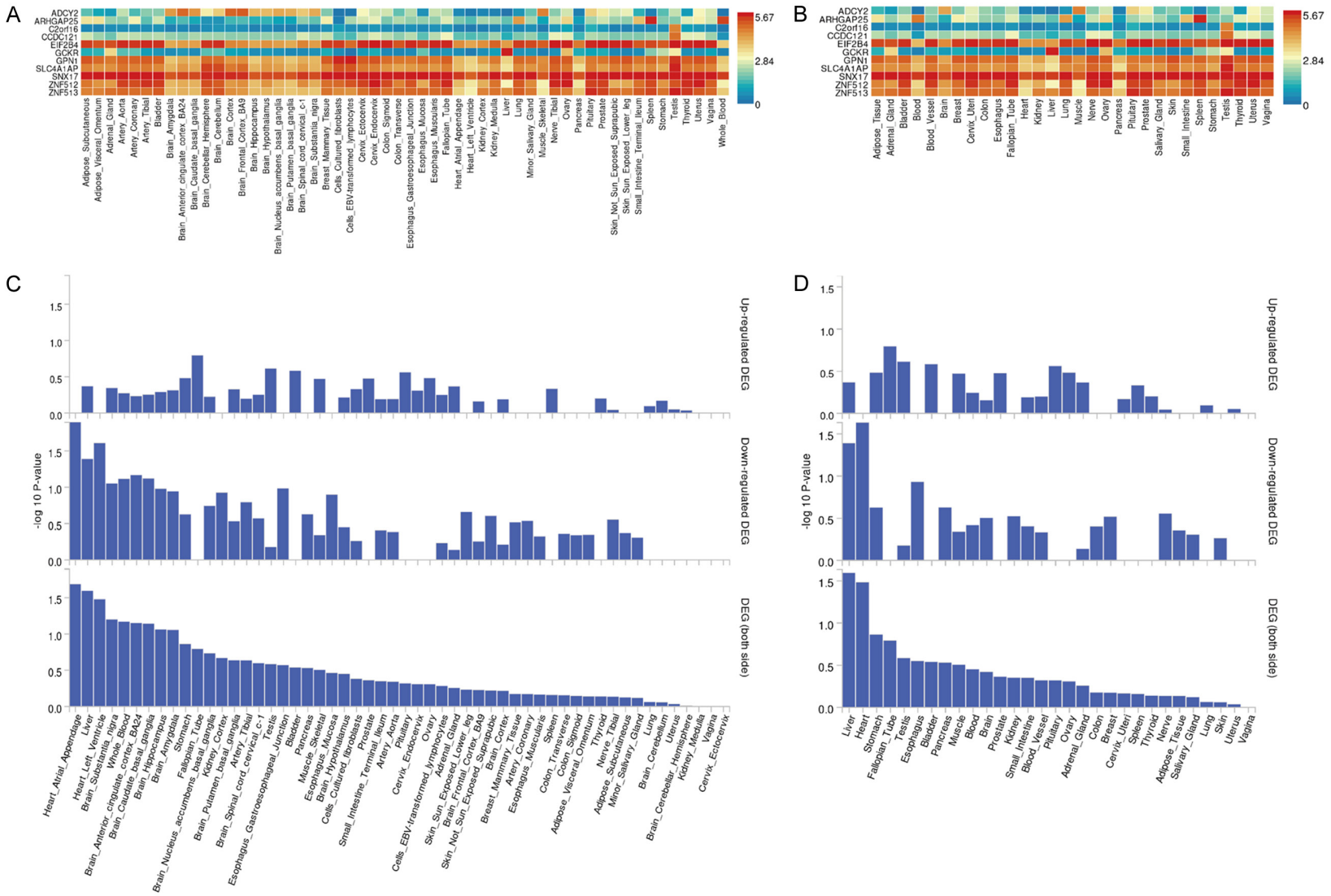

Figure 5. MAGMA tissue-specific analysis of pleiotropy genes. A. Expression of pleiotropic genes in 54 tissues; B. Expression of pleiotropic genes in 30 tissues; C. Up-regulation and down-regulation of pleiotropic genes in 54 tissues; D. Up-regulation and down-regulation of pleiotropic genes in 30 tissues. Multi-marker Analysis of GenoMic Annotation (MAGMA).

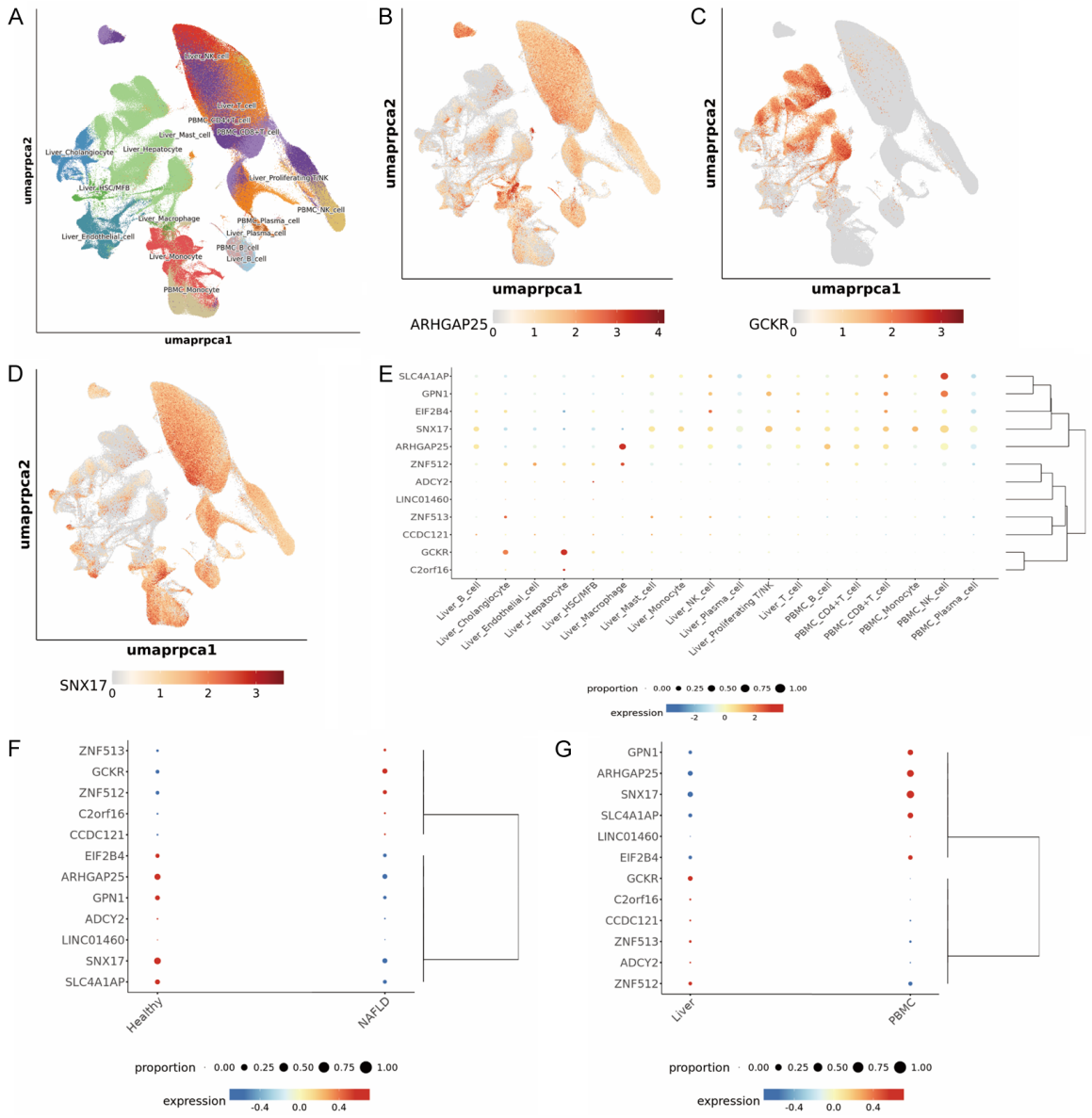

Figure 6. Expression of pleiotropic genes in liver tissues in NAFLD scRNA-seq Database. A. Umap visualization of cell clustering; B. Umap visualization of ARHGAP25 gene expression; C. Umap visualization of GCKR gene expression; D. Umap visualization of SNX17 gene expression; E. Pleiotropic gene expression differences between cell clusters; F. Pleiotropic gene expression differences between NAFLD and healthy controls; G. Pleiotropic gene expression differences between liver and PBMC samples. NAFLD: Non-Alcoholic Fatty Liver Disease, scRNA-seq: Single-cell RNA Sequencing, UMAP: Uniform Manifold Approximation and Projection, ARHGAP25: Rho GTPase Activating Protein 25, GCKR: Glucokinase Regulator, SNX17: Sorting Nexin 17.

tion of the adipogenic pathway (**Figure 7F**). We further explored the correlation between activation scores and clinical measures, revealing that the activation score of pleiotropic genes was significantly negatively correlated with NAFLD disease stage, liver tissue fibrosis, inflammatory activity, and SAF score (P = 0.017, P = 0.023, P = 0.021, P = 0.025, respectively) (**Figure 7G**), which is consistent with the tissue-specific results, suggesting that the overall down-regulation of this group of pleiotropic genes in the liver contributes to the development of fatty liver.

Construction of animal models

The overall timeline and experimental process for constructing the IBS model are presented in **Figure 8A**. During restraint stress induction, mice in the experimental group exhibited pro-

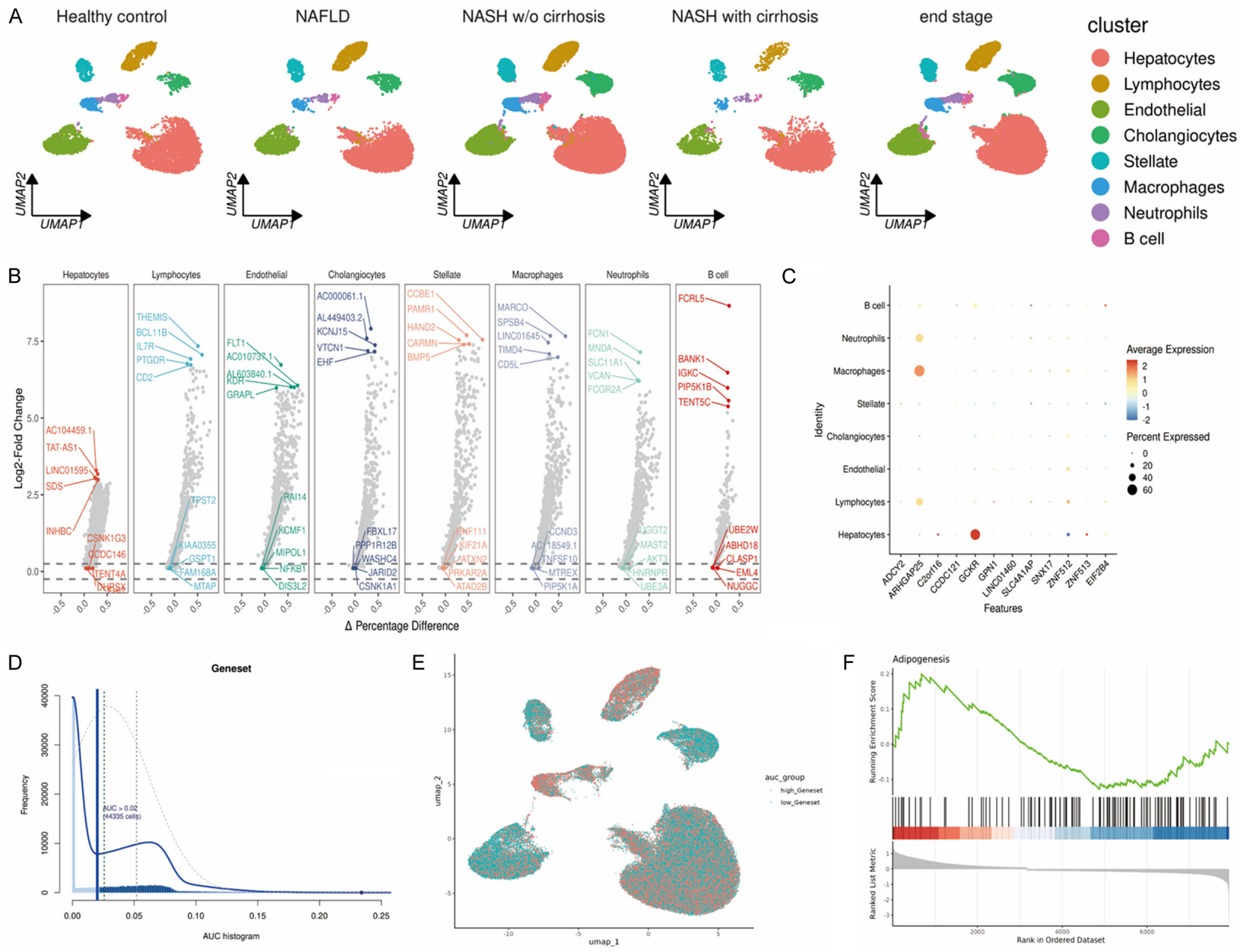
A
Healthy control
NAFLD
NASH w/o cirrhosis
NASH with cirrhosis
end stage
UMAP2
UMAP1
cluster
Hepatocytes
Lymphocytes
Endothelial
Cholangiocytes
Stellate
Macrophages
Neutrophils
B cell
B
Log2-Fold Change
Δ Percentage Difference
C
Identity
Features
Average Expression
Percent Expressed
D
Geneset
Frequency
AUC histogram
E
auc_group
high_Geneset
low_Geneset
umap_1
umap_2
F
Adipogenesis
Running Enrichment Score
Ranked List Metric
Rank in Ordered Dataset

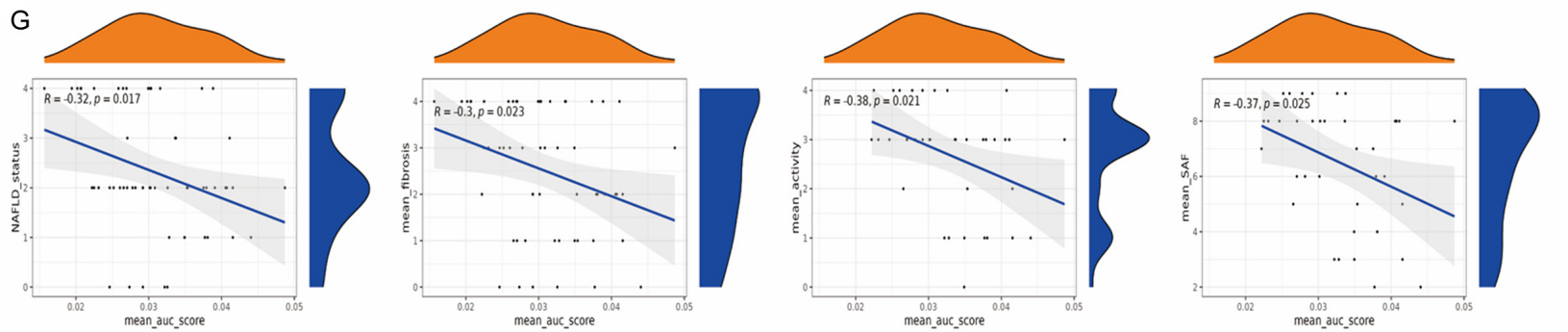

Figure 7. Pleiotropic gene activation score and its association with NAFLD progression. A. Visualization of cell clusters across different stages of NAFLD; B. Marker genes of each cell subsets; C. Expression of pleiotropic genes among cell subsets; D. AUCell thresholds for gene activation scoring; E. High- and low-activation groups based on activation scores; F. Upregulation of adipogenic pathway in the low-activation group; G. Correlation between activation score and disease stage, liver tissue fibrosis, inflammatory activity, and SAF score. NAFLD: Non-Alcoholic Fatty Liver Disease, AUC: Area Under Curve, SAF: Steatosis-Activity-Fibrosis.

gressive weight loss and varying degrees of diarrhea. The first mouse in the second cage of the experimental group died on the first day of the experiment, while the rest of the mice survived until the end of the experiment. To assess weight change differences, standard mixed models, heteroscedasticity-adjusted models, and robust mixed models were constructed using time-weighted data, with time as an interactive variable. All three models indicated significant weight reduction in the experimental group compared to controls (standard mixed model: $\beta = -0.094$, $P < 0.001$; heteroscedasticity-adjusted model: $\beta = -0.094$, $P < 0.001$; robust mixed model: $\beta = -0.095$, $P < 0.001$). However, behavioral analyses revealed non-significant reductions in locomotor activity within central and peripheral zones in the experimental group (**Figure 8B**, **8C**).

Following cervical dislocation, fresh liver tissues were subjected to Oil Red O staining. Control group mice showed no detectable lipid droplet staining, while partial IBS-D mice (n = 2) displayed lipid droplet deposition (**Figure 8D**).

Verification of differences in gene transcriptional expression

RT-qPCR analysis of hepatic gene expression profiles in IBS-D mice was performed after excluding the lncRNA LINC01460 due to a lack of murine homology. Relative quantification ($2^{-\Delta\Delta Ct}$ method, *Actb* as reference gene) was performed on 11 candidate genes (experimental group: n = 7; control group: n = 7). Samples with > 0.5 Ct variation across technical replicates were excluded, and all genes showed downregulation trends consistent with predictions. Significant downregulation trends were observed in *CCDC121* (coiled-coil domain containing 121, P = 0.0236), *GCKR* (glucokinase regulator, P = 0.0041), *GPN1* (GPN-loop GTPase 1, P = 0.0381), *SLC4A1AP* (solute carrier family 4 member 1 adaptor protein, P = 0.0247), and *zfp513* (zinc finger protein 513, P = 0.0091) (**Figure 9A**, **9B**). The functional enrichment and experimental validation results are consolidated in **Figure 9**. The GO analysis for Biological Process (BP) and Molecular Function (MF) is presented as column graphs, providing the functional context for the validation of gene expression (**Figure 9C**).

Verification of protein expression differences

Western blot analysis was performed to evaluate the expression levels of ADCY2, SLC4A1AP, ARHGAP25, ZNF512, GCKR, and GPN1 in the liver tissues of IBS model mice and control mice. The results revealed a marked decrease in the expression of GCKR, GPN1, SLC4A1AP, and ZNF512, whereas no significant alterations were observed in the expression of ADCY2 or ARHGAP25 (**Figure 9D-I**).

Discussion

This study investigated the association and causality between IBS and NAFLD using a comprehensive approach and further explored the common genetic mechanisms of IBS and NAFLD. Initial Mendelian randomization and genetic analyses demonstrated unidirectional susceptibility of IBS patients to NAFLD and identified significant genetic correlations between the two disorders.

The biological functions of the identified pleiotropic genes can be categorized into three core metabolic modules: cyclic adenosine monophosphate (cAMP) signaling, cholesterol metabolism, and glucose metabolism. The convergence on these pathways is highly pertinent to NAFLD pathogenesis. For instance, disrupted glucose metabolism, often characterized by a mismatch between anabolic (e.g., de novo lipogenesis) and catabolic (e.g., β-oxidation) fluxes, is a well-established driver of hepatic steatosis, frequently mediated by insulin resistance [27]. The cAMP signaling pathway, consistently enriched in our analyses, is a critical regulator of both intestinal and hepatic homeostasis. Previous studies have shown that cAMP activation can ameliorate intestinal inflammation by reducing pro-inflammatory cytokines (e.g., IL-1β, TGF-β, TNF-α) in IBS models [28], while in the liver, the cAMP-protein kinase A (PKA) axis is a key modulator of carbohydrate and lipid metabolism [29]. The observed downregulation of cAMP-related genes aligns with previous reports that inhibition of PKA signaling exacerbates hepatic steatosis [30], suggesting that impaired cAMP signaling might represent a common mechanistic link connecting gut dysfunction in IBS to metabolic dysregulation in the liver.

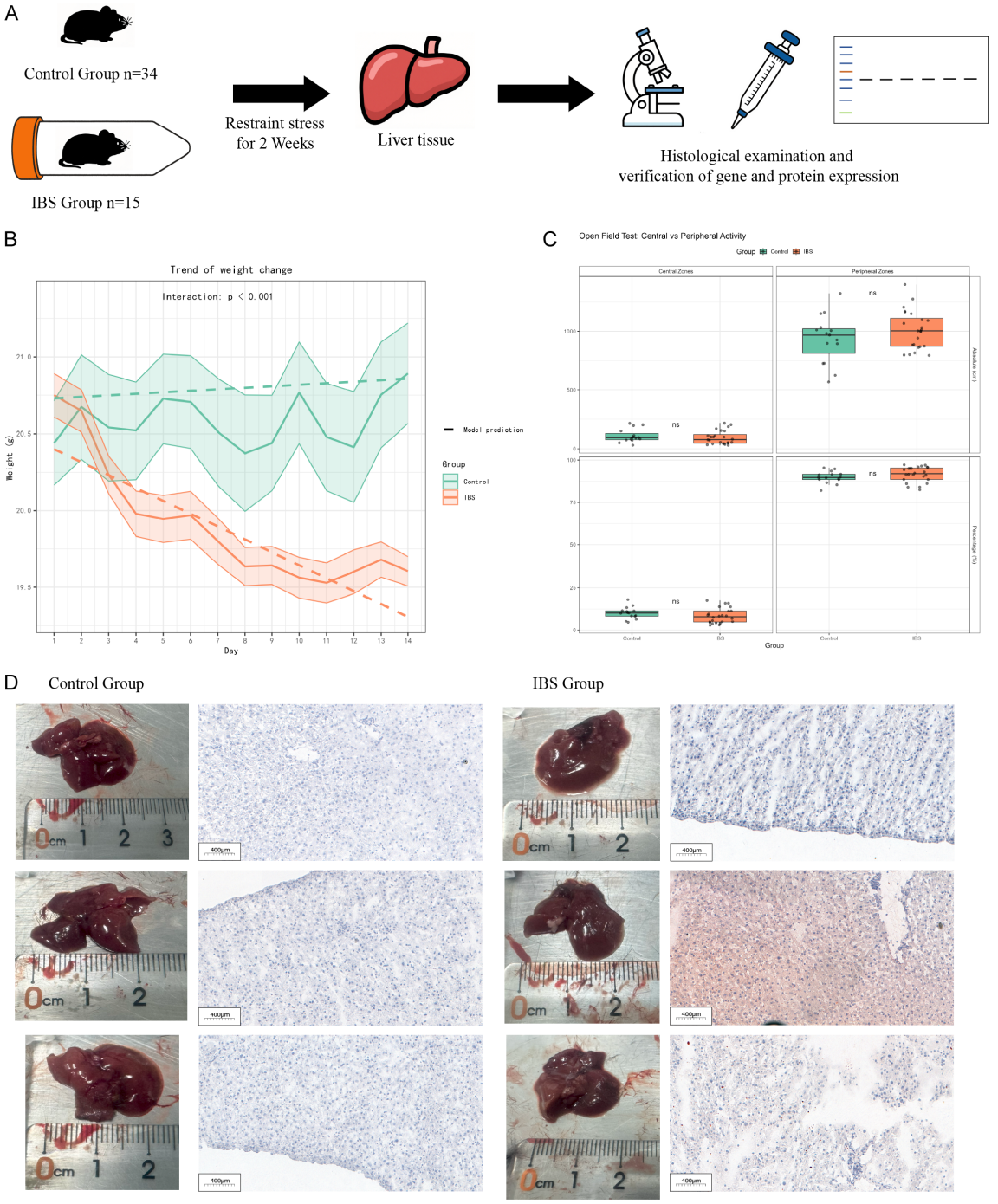

Figure 8. Animal Experiments. A. Treatment protocols for control and IBS groups. IBS mice underwent 14-day restraint stress before subsequent procedures; B. Body weight trajectories; C. Locomotor activity in central vs. peripheral zones during open-field tests; D. Representative hepatic Oil Red O staining (40×). Mild lipid droplet accumulation was observed in a subset of IBS mice, while controls exhibited no stained lipid droplets. IBS: Irritable Bowel Syndrome.

We further localized the action of these pleiotropic genes predominantly to the liver, where they exhibited an overall downregulation trend. This suggests that their reduced expression may predispose IBS patients to NAFLD development. This premise was supported by single-cell RNA sequencing data, which revealed disease state-specific differential expression pat-

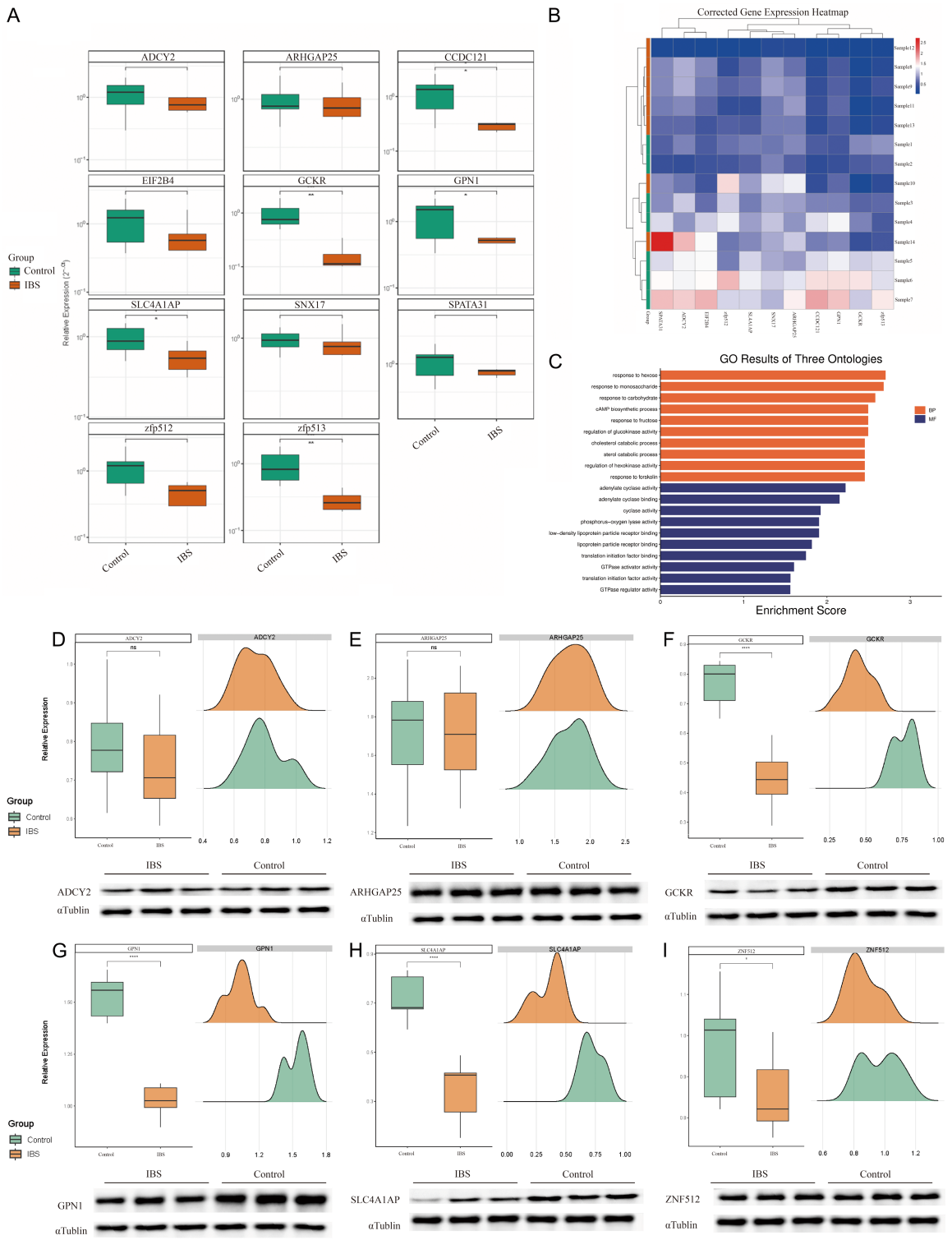

Figure 9. Verification of gene and protein expression. A. Expression of pleiotropic genes detected by RT-qPCR (n = 7/group); B. Heat map of the expression of the pleiotropic genes in IBS group; C. GO enrichment analysis of pleiotropic genes in terms of biological process and molecular functions; D-I. Differences in protein expression of six target genes. IBS: Irritable Bowel Syndrome, NAFLD: Non-Alcoholic Fatty Liver Disease, RT-qPCR: reverse transcription quantitative polymerase chain reaction, CCDC121: Coiled-Coil Domain Containing 121, GCKR: Glucokinase Regulator, GPN1: GPN-Loop GTPase 1, SLC4A1AP: SLC4A1 Associated Pseudogene, Zfp513: Zinc Finger Protein 513, ARHGAP25: Rho GTPase Activating Protein 25, ZNF512: Zinc Finger Protein 512.

terns. The functional relevance of this coordinated downregulation was underscored by our activation score analysis. A lower activation score, indicative of diminished protective gene expression, was associated with the upregulation of lipogenic pathways and, more critically, correlated inversely with NAFLD disease stage, hepatic fibrosis, inflammatory activity, and SAF scores. These findings strongly indicate that these pleiotropic genes collectively exert a protective effect against NAFLD progression.

To experimentally validate our genetic findings, we established an IBS animal model. The successful induction was evidenced by phenotypic changes, including loose stools and weight loss. Subsequent pathological examination revealed hepatic lipid droplet deposition in a subset of IBS mice. At the molecular level, RT-qPCR and western blot analyses of liver tissues confirmed significant downregulation of several key pleiotropic genes, including GCKR, GPN1, SLC4A1AP, and ZNF512, corroborating the downregulation trend observed in human genetic and transcriptomic analyses.

The specific roles of these downregulated genes further illuminate their potential involvement in metabolic dysregulation. GCKR, primarily expressed in hepatocytes, regulates glucokinase activity; its polymorphism is known to impair this regulation, leading to enhanced hepatic glucose uptake and lipid accumulation, and is significantly associated with NAFLD and other metabolic diseases [31, 32]. The observed reduction in GCKR expression aligns with this pro-steatotic mechanism. Similarly, ARHGAP25, enriched in macrophages, functions as a negative regulator of phagocytosis. Its downregulation, as seen in our model, may enhance phagocytic activity and associated oxidative stress [33], implicating macrophage dysregulation in the IBS-NAFLD axis. Other genes like ZNF512 (https://www.genecards.org/cgi-bin/carddisp.pl?gene=ZNF512&keywords=ZNF512) and CCDC121 (https://www.genecards.org/cgi-bin/carddisp.pl?gene=CCDC121&keywords=CCDC121) have also been linked to lipid metabolism disorders and familial hypercholesterolemia in prior reports, suggesting that their concerted downregulation may contribute to the metabolic phenotype observed. The case of C2orf16/SPATA31H1, which has been associated with NAFLD and metabolic syndrome [34], further reinforces the notion that the pleiotropic genes we identified are enmeshed in a network of metabolic regulation.

Our findings have several limitations. First, although the LDSC method revealed shared genetic architecture between IBS and NAFLD, future replication studies are required to mitigate potential false-positive associations. Second, while results were validated in single-cell datasets and our activation scoring system, the hepatic-specific validation precludes definitive conclusions about these genes' roles in extrahepatic tissues, limiting interpretability. Finally, as the GWAS datasets were derived from European populations, the generalizability of IBS-NAFLD associations to other ancestries remains unverified. Therefore, additional multi-ethnic cohorts and functional validation across tissues are needed to fully elucidate the pathophysiologic links between these conditions.

Conclusion

This study demonstrated a genetic association and a causal relationship between IBS and NAFLD. We identified twelve pleiotropic genes that were consistently downregulated. Functional analyses indicate that these genes are involved in cAMP signaling, cholesterol metabolism, and glucose metabolism. The downregulation of these genes was associated with more severe NAFLD in clinical cohorts and was confirmed in an experimental animal model. These results provide a genetic explanation for the elevated risk of NAFLD in IBS patients. The identified genes and pathways constitute candidates for future research into the mechanisms linking these two conditions.

Acknowledgements

We sincerely thank the researchers who have provided us with guidance and advice. The publication fee of this study was supported by the "Pioneer" and "Leading Goose" R&D Program of Zhejiang Province (2023C03050).

Disclosure of conflict of interest

None.

Abbreviations

ADCY2, Adenylate Cyclase 2; ARHGAP25, Rho GTPase Activating Protein 25; C2orf16/

SPATA31H1, Chromosome 2 Open Reading Frame 16/Spermatogenesis Associated 31 Member H1; CCDC121, Coiled-Coil Domain Containing 121; GCKR, Glucokinase Regulator; GPN1, GPN-Loop GTPase 1; LINC01460, Long Intergenic Non-Protein Coding RNA 1460; SLC4A1P, SLC4A1 Pseudogene; SNX17, Sorting Nexin 17; ZNF512, Zinc Finger Protein 512; ZNF513, Zinc Finger Protein 513; EIF2B4, Eukaryotic Translation Initiation Factor 2B Subunit Beta; zfp512, zinc finger protein 512; zfp513, zinc finger protein 513; IBS, Irritable Bowel Syndrome; NAFLD, Non-Alcoholic Fatty Liver Disease; NASH, Non-alcoholic Steatohepatitis; MR, Mendelian randomization; LDSC, LD Score regression; PLACO, Pleiotropy Analysis with Collapsing; coloc, colocalization; MAGMA, Multi-marker Analysis of GenoMic Annotation; FDR, false discovery rate; GO, Gene Ontology; KEGG, Kyoto Encyclopedia of Genes and Genomes; MF, Molecular Function; BP, Biological Process; CC, Cellular Component; IVW, inverse-variance weighted; MASLD, Metabolic Dysfunction-Associated Fatty Liver Disease; GWAS, Genome-wide association study; NHGRI, National Human Genome Research Institute; EBI, European Bioinformatics Institute; SNP, Single Nucleotide Polymorphism; US, United States; FUMA, Functional Mapping and Annotation; scRNA-seq, Single-cell RNA Sequencing; PCA, Principal Component Analysis; UMAP, Uniform Manifold Approximation and Projection; AUC, Area Under Curve; OFT, Open Field Test; RT-qPCR, reverse transcription quantitative polymerase chain reaction; PVDF, polyvinylidene fluoride; GABA, Gamma-aminobutyric acid; cAMP, cyclic adenosine monophosphate; PKA, protein kinase A; GSEA, Gene Set Enrichment Analysis; SAF, Steatosis-Activity-Fibrosis.

Address correspondence to: Bin Lv, Department of Gastroenterology, The First Affiliated Hospital of Zhejiang Chinese Medical University (Zhejiang Provincial Hospital of Traditional Chinese Medicine), 54 Youdian Road, Hangzhou, Zhejiang, China. E-mail: lvbin@medmail.com.cn

References

[1] Takeoka A, Kimura T, Hara S, Hamaguchi T, Fukudo S and Tayama J. Prevalence of irritable bowel syndrome in Japan, China, and South Korea: an international cross-sectional study. J Neurogastroenterol Motil 2023; 29: 229-237.

[2] Zhang L, Wang HL, Zhang YF, Mao XT, Wu TT, Huang ZH, Jiang WJ, Fan KQ, Liu DD, Yang B, Zhuang MH, Huang GM, Liang Y, Zhu SJ, Zhong JY, Xu GY, Li XM, Cao Q, Li YY and Jin J. Stress triggers irritable bowel syndrome with diarrhea through a spermidine-mediated decline in type I interferon. Cell Metab 2025; 37: 87-103, e10.

[3] Staudacher HM, Black CJ, Teasdale SB, Mikocka-Walus A and Keefer L. Irritable bowel syndrome and mental health comorbidity - approach to multidisciplinary management. Nat Rev Gastroenterol Hepatol 2023; 20: 582-596.

[4] Li Z, Ma Q, Deng Y, Rolls ET, Shen C, Li Y, Zhang W, Xiang S, Langley C, Sahakian BJ, Robbins TW, Yu JT, Feng J and Cheng W. Irritable bowel syndrome is associated with brain health by neuroimaging, behavioral, biochemical, and genetic analyses. Biol Psychiatry 2024; 95: 1122-1132.

[5] Mayer EA, Ryu HJ and Bhatt RR. The neurobiology of irritable bowel syndrome. Mol Psychiatry 2023; 28: 1451-1465.

[6] Lee HH, Lee HA, Kim EJ, Kim HY, Kim HC, Ahn SH, Lee H and Kim SU. Metabolic dysfunction-associated steatotic liver disease and risk of cardiovascular disease. Gut 2024; 73: 533-540.

[7] Sanyal AJ, Foucquier J, Younossi ZM, Harrison SA, Newsome PN, Chan WK, Yilmaz Y, De Ledinghen V, Costentin C, Zheng MH, Wai-Sun Wong V, Elkhashab M, Huss RS, Myers RP, Roux M, Labourdette A, Destro M, Fournier-Poizat C, Miette V, Sandrin L and Boursier J. Enhanced diagnosis of advanced fibrosis and cirrhosis in individuals with NAFLD using fibroscan-based agile scores. J Hepatol 2023; 78: 247-259.

[8] Foerster F, Gairing SJ, Müller L and Galle PR. NAFLD-driven HCC: safety and efficacy of current and emerging treatment options. J Hepatol 2022; 76: 446-457.

[9] Wong VW, Ekstedt M, Wong GL and Hagström H. Changing epidemiology, global trends and implications for outcomes of NAFLD. J Hepatol 2023; 79: 842-852.

[10] Ng JJJ, Loo WM and Siah KTH. Associations between irritable bowel syndrome and non-alcoholic fatty liver disease: a systematic review. World J Hepatol 2023; 15: 925-938.

[11] Purssell H, Bennett L, Street O, Hanley KP, Hanley N, Vasant DH and Athwal VS. The prevalence and burden of Rome IV bowel disorders of gut brain interaction in patients with non-alcoholic fatty liver disease: a cross-sectional study. Sci Rep 2023; 13: 8769.

[12] Dean YE, Loayza Pintado JJ, Rouzan SS, Nale LL, Abbas A, Aboushaira A, Alkasajy F, Ghanem AA, Patil VM, Gordeyeva Y, Motawea KR, Le MLP, Galal A, Cicani L, Attta R, Soliman A, Alzabidi L, Subedi A, Anjum N, Nahedh A, Mady T, Hazimeh Y, Amin H and Aiash H. The relationship between irritable bowel syndrome and metabolic syndrome: a systematic review and meta-analysis of 49,662 individuals. Endocrinol Diabetes Metab 2025; 8: e70041.

[13] Zhai L, Xiao H, Lin C, Wong HLX, Lam YY, Gong M, Wu G, Ning Z, Huang C, Zhang Y, Yang C, Luo J, Zhang L, Zhao L, Zhang C, Lau JY, Lu A, Lau LT, Jia W, Zhao L and Bian ZX. Gut microbiota-derived tryptamine and phenethylamine impair insulin sensitivity in metabolic syndrome and irritable bowel syndrome. Nat Commun 2023; 14: 4986.

[14] Vonderlin J, Chavakis T, Sieweke M and Tacke F. The multifaceted roles of macrophages in NAFLD pathogenesis. Cell Mol Gastroenterol Hepatol 2023; 15: 1311-1324.

[15] Smith GD and Ebrahim S. Mendelian randomization: prospects, potentials, and limitations. Int J Epidemiol 2004; 33: 30-42.

[16] Camargo Tavares L, Lopera-Maya EA, Bonfiglio F, Zheng T, Sinha T, Zanchetta Marques F, Zhernakova A, Sanna S and D'Amato M. Rome III criteria capture higher irritable bowel syndrome SNP-heritability and highlight a novel genetic link with cardiovascular traits. Cell Mol Gastroenterol Hepatol 2024; 18: 101345.

[17] Ghodsian N, Abner E, Emdin CA, Gobeil É, Taba N, Haas ME, Perrot N, Manikpurage HD, Gagnon É, Bourgault J, St-Amand A, Couture C, Mitchell PL, Bossé Y, Mathieu P, Vohl MC, Tchernof A, Thériault S, Khera AV, Esko T and Arsenault BJ. Electronic health record-based genome-wide meta-analysis provides insights on the genetic architecture of non-alcoholic fatty liver disease. Cell Rep Med 2021; 2: 100437.

[18] Bulik-Sullivan BK, Loh PR, Finucane HK, Ripke S, Yang J; Schizophrenia Working Group of the Psychiatric Genomics Consortium; Patterson N, Daly MJ, Price AL and Neale BM. LD score regression distinguishes confounding from polygenicity in genome-wide association studies. Nat Genet 2015; 47: 291-295.

[19] Tanha HM and Sathyanarayanan A; International Headache Genetics Consortium, Nyholt DR. Genetic overlap and causality between blood metabolites and migraine. Am J Hum Genet 2021; 108: 2086-2098.

[20] de Leeuw CA, Mooij JM, Heskes T and Posthuma D. MAGMA: generalized gene-set analysis of GWAS data. PLoS Comput Biol 2015; 11: e1004219.

[21] Ma W, Zhong X, Cai B, Shao M, Yu X, Lv M, Xu S, Zhan B, Li Q, Ma M, Kjær M B, Huang J, Luo Y, Grønbæk H and Lin L. Unveiling the pathogenesis of non-alcoholic fatty liver disease by decoding biomarkers through integrated single-cell and single-nucleus profiles. 2023; 2023.10.05.23296635.

[22] Gribben C, Galanakis V, Calderwood A, Williams EC, Chazarra-Gil R, Larraz M, Frau C, Puengel T, Guillot A, Rouhani FJ, Mahbubani K, Godfrey E, Davies SE, Athanasiadis E, Saeb-Parsy K, Tacke F, Allison M, Mohorianu I and Vallier L. Acquisition of epithelial plasticity in human chronic liver disease. Nature 2024; 630: 166-173.

[23] Stuart T, Butler A, Hoffman P, Hafemeister C, Papalexi E, Mauck WM 3rd, Hao Y, Stoeckius M, Smibert P and Satija R. Comprehensive integration of single-cell data. Cell 2019; 177: 1888-1902, e21.

[24] Bucci M. Choosing a mating site. Nat Chem Biol 2019; 15: 1131.

[25] Aibar S, González-Blas CB, Moerman T, Huynh-Thu VA, Imrichova H, Hulselmans G, Rambow F, Marine JC, Geurts P, Aerts J, van den Oord J, Atak ZK, Wouters J and Aerts S. SCENIC: single-cell regulatory network inference and clustering. Nat Methods 2017; 14: 1083-1086.

[26] Liberzon A, Birger C, Thorvaldsdóttir H, Ghandi M, Mesirov JP and Tamayo P. The molecular signatures database (MSigDB) hallmark gene set collection. Cell Syst 2015; 1: 417-425.

[27] Bhat N and Mani A. Dysregulation of lipid and glucose metabolism in nonalcoholic fatty liver disease. Nutrients 2023; 15: 2323.

[28] Chao G and Zhang S. Aquaporins 1, 3 and 8 expression and cytokines in irritable bowel syndrome rats' colon via cAMP-PKA pathway. Int J Clin Exp Pathol 2018; 11: 4117-4123.

[29] Sen K, Bhattacharyya D, Sarkar A, Das J, Maji N, Basu M, Ghosh Z and Ghosh TC. Exploring the major cross-talking edges of competitive endogenous RNA networks in human chronic and acute myeloid leukemia. Biochim Biophys Acta Gen Subj 2018; 1862: 1883-1892.

[30] Yang J, Zhang X, Yi L, Yang L, Wang WE, Zeng C, Mi M and Chen X. Hepatic PKA inhibition accelerates the lipid accumulation in liver. Nutr Metab 2019; 16: 69.

[31] Li J, Zhao Y, Zhang H, Hua W, Jiao W, Du X, Rui J, Li S, Teng H, Shi B, Yang X and Zhu L. Contribution of Rs780094 and Rs1260326 polymorphisms in GCKR gene

to non-alcoholic fatty liver disease: a meta-analysis involving 26,552 participants. Endocr Metab Immune Disord Drug Targets 2021; 21: 1696-1708.

[32] Eslam M, Valenti L and Romeo S. Genetics and epigenetics of NAFLD and NASH: clinical impact. J Hepatol 2018; 68: 268-279.

[33] Csépányi-Kömi R, Sirokmány G, Geiszt M and Ligeti E. ARHGAP25, a novel Rac GTPase-activating protein, regulates phagocytosis in human neutrophilic granulocytes. Blood 2012; 119: 573-582.

[34] Anstee QM, Darlay R, Cockell S, Meroni M, Govaere O, Tiniakos D, Burt AD, Bedossa P, Palmer J, Liu YL, Aithal GP, Allison M, Yki-Järvinen H, Vacca M, Dufour JF, Invernizzi P, Prati D, Ekstedt M, Kechagias S, Francque S, Petta S, Bugianesi E, Clement K, Ratziu V, Schattenberg JM, Valenti L, Day CP, Cordell HJ and Daly AK; EPoS Consortium Investigators. Genome-wide association study of non-alcoholic fatty liver and steatohepatitis in a histologically characterised cohort☆. J Hepatol 2020; 73: 505-515.

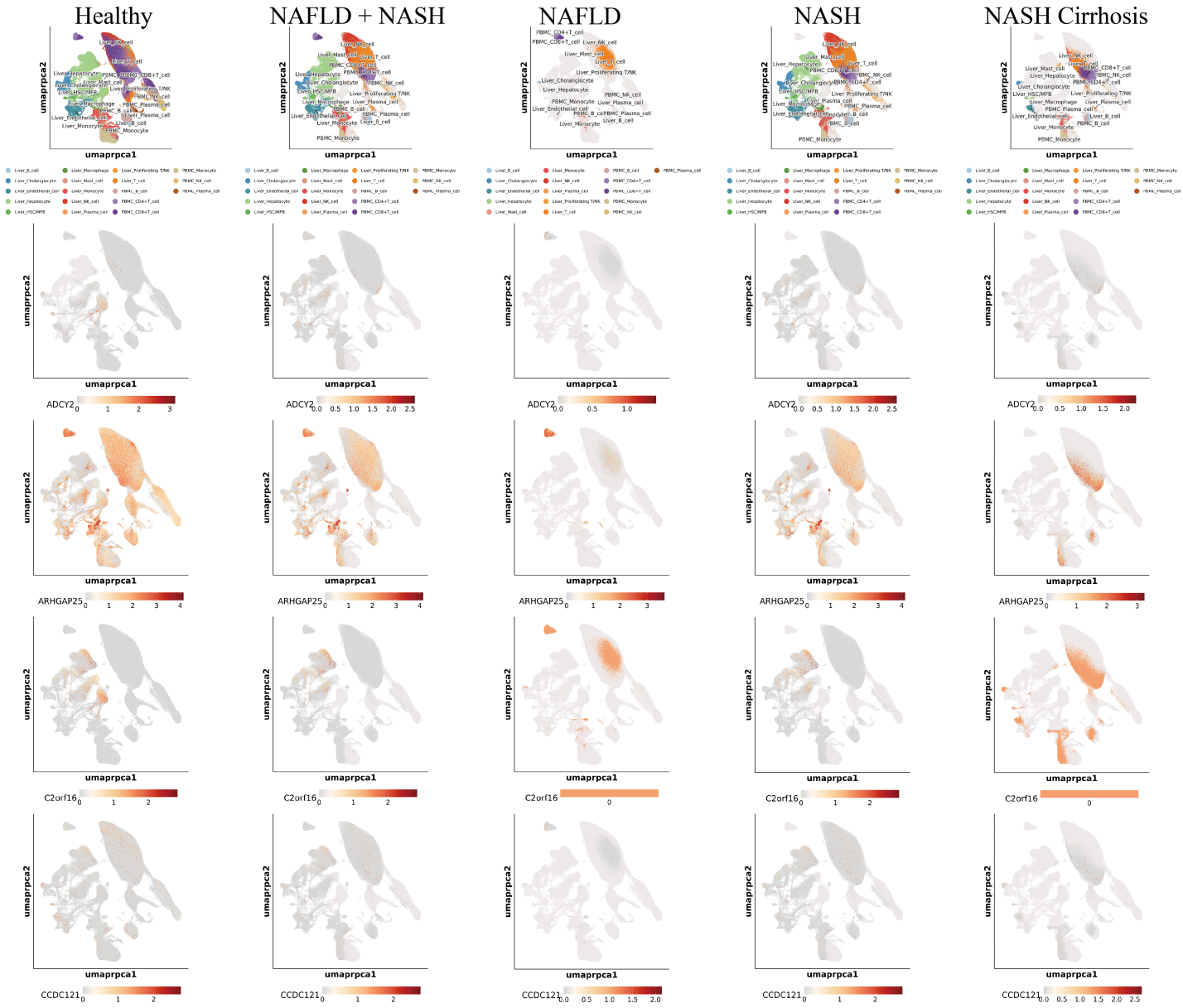
Healthy
NAFLD + NASH
NAFLD
NASH
NASH Cirrhosis
ADCY2
ARHGAP25
C2orf16
CCDC121
umaprpca1
umaprpca2

Genetic correlation of IBS and NAFLD

EIF2B4

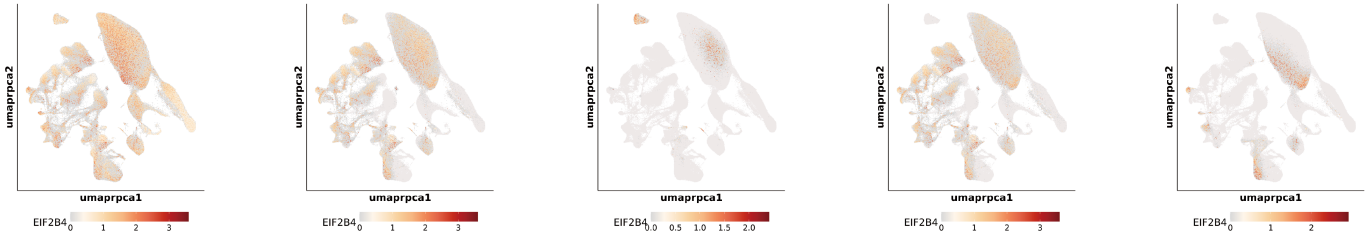

GCKR

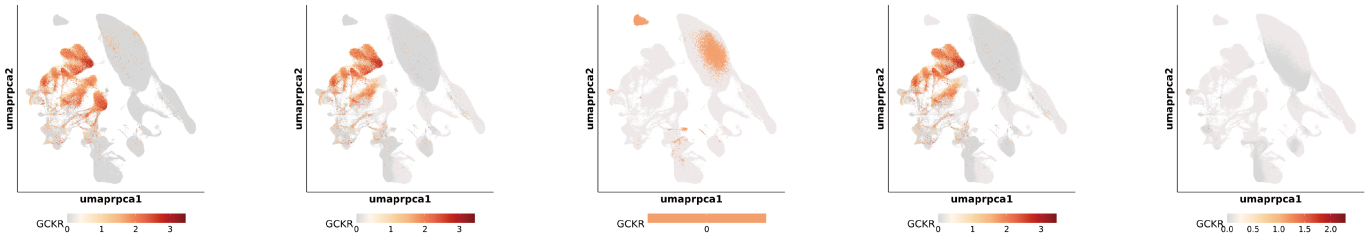

GPN1

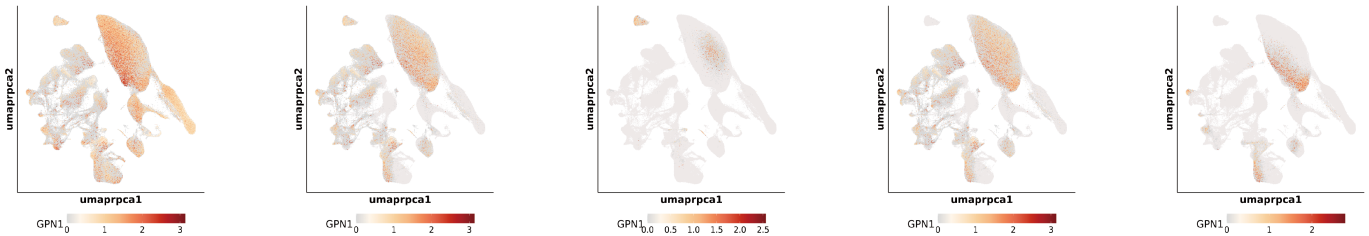

LINC01460

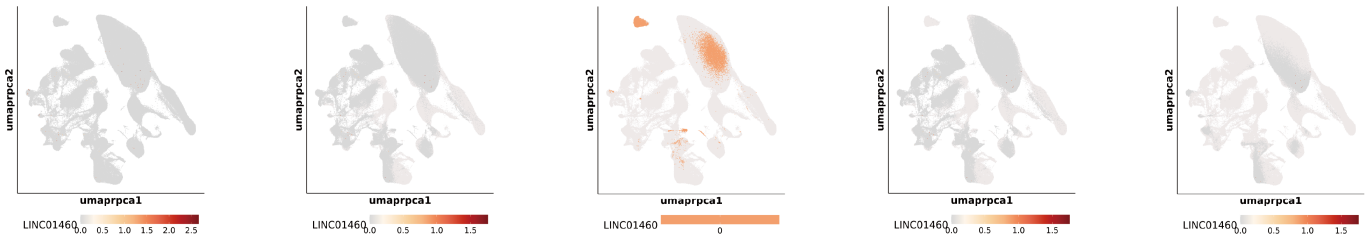

SLC4A1AP

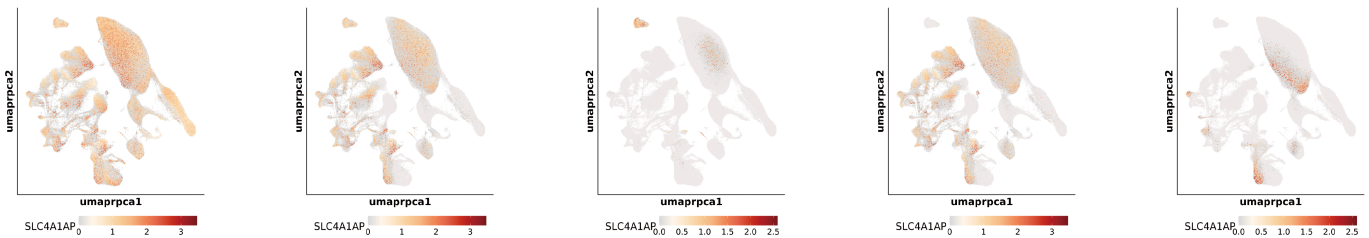

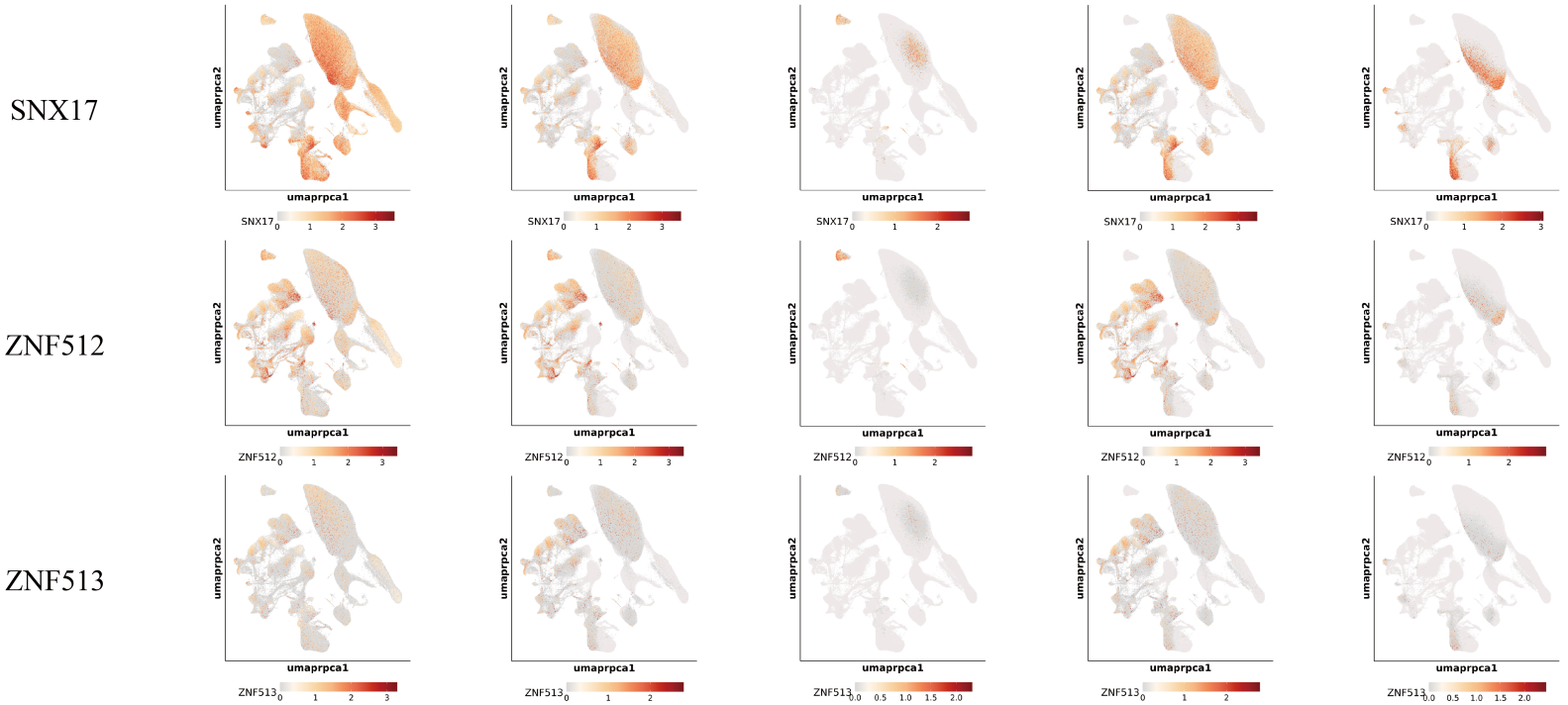

Supplementary Figure 1. Expression patterns of pleiotropic genes across NAFLD clinical spectra in liver tissue. Gene expression levels (*ADCY2, ARHGAP25, C2orf16, CCDC121, GCKR, GPN1, LINC01460, SLC4A1AP, SNX17, ZNF512, ZNF513,* and *EIF2B4*) are compared across five groups: Healthy controls, NAFLD+NASH, NAFLD, NASH, and NASH cirrhosis. Data were derived from the NAFLD scRNA-seq database Each subpanel illustrates the expression distribution of one gene across the disease states. ADCY2, Adenylate Cyclase 2; ARHGAP25, Rho GTPase Activating Protein 25; C2orf16, Chromosome 2 Open Reading Frame 16; CCDC121, Coiled-Coil Domain Containing 121; GCKR, Glucokinase Regulator; GPN1, GPN-Loop GTPase 1; LINC01460, Long Intergenic Non-Protein Coding RNA 1460; SLC4A1P, SLC4A1 Pseudogene; SNX17, Sorting Nexin 17; ZNF512, Zinc Finger Protein 512; ZNF513, Zinc Finger Protein 513; EIF2B4, Eukaryotic Translation Initiation Factor 2B Subunit Beta; NAFLD, Non-Alcoholic Fatty Liver Disease; NASH, Nonalcoholic Steatohepatitis; scRNA-seq, Single-cell RNA Sequencing.